Exploring the genetics and physiology underlying the non-photochemical quenching phenotype of the Ely nucleus

Justine Drouault
Master Plant Sciences, Plant Breeding and Genetics
Major thesis, Laboratory of Genetics
Second half of 2019
Supervisors: Tom Theeuwen and Mark Aarts
Examiners: Tom Theeuwen and Bas Zwaan
Student number: 960423200100

WAGENINGEN
UNIVERSITY & RESEARCH

Table of content

Abstract

During time scales, ranging from a day to a season, plants, as sessile organisms, are constantly exposed to light intensity fluctuations. A long exposure, to what plants perceive as high light intensities are harmful to them. Then, plants have developed photoprotection mechanisms particularly non-photochemical quenching (NPQ). However, when the light intensity decreases, NPQ is impeding photosynthesis efficiency (ϕPSII). If the NPQ mechanism was faster to relax when the light intensity decreases, photosynthesis could be more efficient, but, a too fast relaxing NPQ could be harmful to the plant. The plasticity of the NPQ phenotype has been studied on a cytoplasmic swap panel made from seven *Arabidopsis thaliana* accessions. The Ely nucleus was giving a higher NPQ, while the chloroplast genome of Ely was giving a lower rate of ϕPSII due to a *psbA* mutation. Remarkably, in Ely, the higher NPQ has been correlated with the increase of the NPQ fast-relaxing component (qE). In this thesis, we investigate whether the NPQ phenotype of Ely nucleus, could be beneficial for the plant and whether it was an adaptation to *psbA* mutation or was present before it. A cybrid population composed of Ely_{Col} , Col_{Col}, and Hun_{Col} was used, and a fluctuating light response curve and an NPQ relaxation experiment were realised. Hun has the *psbA* mutated gene but a different nucleus of Ely, hence, its NPQ phenotype was compared with the Ely nucleus NPQ phenotype. This step aimed to get insights into the origin of El nucleic variation. From the results of the fluctuating light response curve, Hun did not present the same NPQ phenotype, impeding our conclusion on Ely nucleic origin. The results of both experiments were that, under fluctuating light conditions, NPQ phenotype of Ely nucleus by relaxing faster was less impeding ϕPSII and seems a beneficial trait under these conditions.

1 Introduction

In the coming decades, human food production will have to face two major challenges, global climate change, and population growth. It is predicted that by 2050 the demand in basic food products will increase by 87% (Ray et al. 2013), while climate change is expected to have a negative impact on the yield by modifying the growing conditions of the crops (Anon 2009). To come up with an increase in crop yield by 100-110% (Tilman et al. 2011) under changing climatic conditions, new crop production systems need to be established (Anon 2009; Kromdijk and Long 2016). Monteith created a model in which he decomposed the harvestable yield in four components: the irradiance, the interception of irradiance, the efficiency of conversion of intercepted irradiance into biomass, and the harvest index (Long et al. 2006; Monteith 1977). In the past decade, according to Monteith's model, the objectives of the breeding programs were to increase the harvest index and the light capture efficiency of the canopy. This has been successfully achieved and these traits are now reaching their biological limit. However, the harvestable yield can still be increased by improving the third parameter, the efficiency of conversion of intercepted irradiance into biomass collectively called photosynthesis (Long et al. 2006).

Photosynthesis is the mechanism on which all life on the planet depends upon. This process is employed by plants and algae to convert CO_2 and H_2O into carbohydrates and O_2 by using light energy (Eq. 1). It starts in the thylakoid membrane, located in the chloroplast (Pessarakli 2005). The process of photosynthesis begins with the absorption of a photon (solar energy) by pigments molecules attached to proteins embedded in the thylakoid's membranes and called light-harvesting complexes (LHCs). The LHCs are used by the plant to collect and concentrate the sunlight energy that will be then transferred towards the reaction center (RC) (a special pair of redox-active chlorophyll molecules). The LHCs and RC form what is called a photosystem (Murchie and Niyogi 2011). There are two types of photosystems in higher plants, photosystem I (PSI) and photosystem II (PSII) (Ballottari et al. 2012; Gao et al. 2018). When the RC receives energy from LHCs, an electron is emitted through the oxidation of specific chlorophyll pigments. This electron is transmitted to a primary quinone electron acceptor Q_A which gets reduced and cannot accept another electron until it transfers the one it gets (Cleland, Melis, and Neale 1986). Then, the electron accepted by Q_A is transferred to other protein complexes and serves to produce the energy needed to fix CO_2 (Figure 1). This mechanism is called photochemistry (Cleland et al. 1986). The photochemistry pathway is essential for the plant as it is the origin of the carbohydrate's formation. The amount of photochemistry can be estimated by the efficiency of the PSII (ϕPSII) (Maxwell and Johnson 2000). ϕPSII is maximal when all the Q_A are oxidized and can receive and transfer electron in the photochemistry pathway, and minimal when all the Q_A are reduced. Q_A oxidized can also be reported as the openness of the RC and Q_A reduced as the closure of the RC (Maxwell and Johnson 2000).

Eq. 1: $H_2O + light + CO_2 \rightarrow CH_2O + O_2$

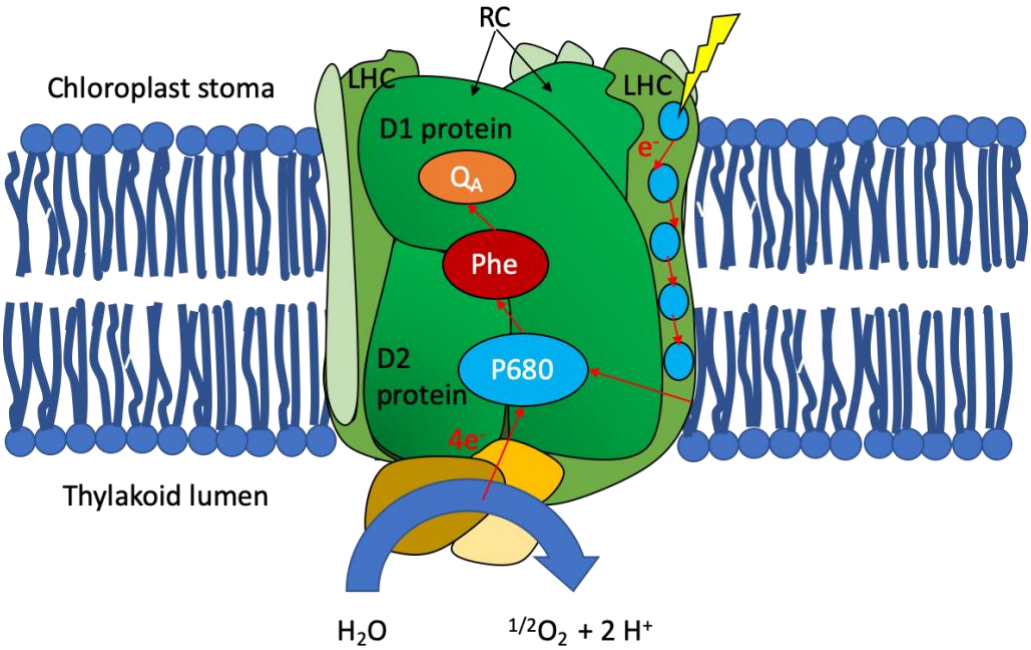

Figure 1: When the light reaches the LHC it is captured by chlorophyll pigments that emit electron energy. This electron energy is then transferred to two specifics chlorophyll molecules (P_{680}) located in the RC. When P_{680} receive sunlight and water electrons, they get oxidized and emits one electron. The electron resulting in the oxidation of P_{680} is transferred to an intermediate primary electron acceptor pheophytin (Phe) and next to a bound primary quinone electron acceptor Q_A which gets reduced. Q_A will then transfer this electron energy to other protein complexes embedded in the thylakoid membrane this is the first step of the photochemistry pathway.

The efficiency of conversion of intercepted irradiance into biomass or the photosynthesis efficiency is defined as the amount of light required by photochemistry to fix a unit of CO_2 (Zhu, Long, and Ort 2010). On time scales going from days to seasons, the light intensity fluctuates due to changes in solar irradiance, clouds, and canopy's leaves movements. Therefore, the amount of light captured by the plant is also fluctuating. When the plant is reached by what a leaf perceives as high light intensity, more energy is allocated to the RC, then, the number of Q_A available to receive energy decreases. A consequence of the decrease of Q_A availability is that the light energy captured by the plant cannot be used anymore in the photochemistry pathway (Külheim, Ågren, and Jansson 2002). Then, the light energy gets accumulated in excess, and chlorophyll molecules have to release their energy by producing a singlet oxygen molecule ($^1O_2$). This phenomenon is called photoinhibition and is detrimental for the plants as $^1O_2$ is a reactive oxygen species (ROS). ROS are harmful to the plant because they break bonds in proteins. The break-up of proteins essential for photosynthesis can ultimately lead to the inactivation of PSII (Foyer and Shigeoka 2011; Müller, Li, and Niyogi 2001). As the plants are sessile organisms their ability to adapt their photosynthetic metabolism to a variable light intensity environment and particularly to high light intensity is crucial for their survival. Therefore, to protect themselves under high light intensity by avoiding the production of ROS and further their damage on cells, plants employ several protective

mechanisms, collectively called photoprotection. These mechanisms help to dissipate the chlorophyll excitation in excess and thus prevent the plant from ROS production and further damages (Müller et al. 2001).

There are two mechanisms of photoprotection by which chlorophyll can return to its steady-state, without producing a singlet oxygen molecule $_1O_2$: non-photochemical quenching (NPQ) and chlorophyll fluorescence (Figure 2). They respectively enable the dissipation of the energy in excess as heat and light (Figure 2) (Anon 2018). The excess of energy loss by chlorophyll fluorescence is low 0.6%-3%, but it is used to measure the activity of photochemistry (Box 1) (Krause and Weis 1991). Under high light intensities, NPQ is the main mechanism by which energy in excess is realised (Horton and Hague 1988). NPQ depends on the ratio $\phi NO/\phi NPQ$, where ϕNO is known as the sum of non-regulated heat dissipation and fluorescence emission, and ϕNPQ as the regulated thermal energy dissipation linked to NPQ. The formation of NPQ induces conformational changes in LHCs which enable the dissipation of energy as heat (Müller et al. 2001).

The formation and relaxation of NPQ are driven by three mechanisms corresponding to different relaxation kinetics qE, qT, and qI (Müller et al. 2001; Zaks et al. 2012). The first one is the fast-relaxing mechanism called qE. This mechanism depends on two phenomena; the ΔpH across the thylakoid membrane and the presence of PSII subunit PsbS (Demmig-Adams et al. 2014). When the pH within the thylakoids membranes decreases due to an H^+ accumulation caused by an increase of the electron transport chain, qE gets activated through the protonation of the PSII proteins (including PsbS) and the conversion of violaxanthin to zeaxanthin by the violaxanthin deepoxidase (VDE) (Müller et al. 2001; Zaks et al. 2012). When the light intensity decreases, half of the conformational changes induced in qE mechanisms will be back to their relaxed form after 30 seconds. The qT process is slower to relax, from one to ten minutes. However, the effects of qT are almost inexistent in higher plants, so they were not the object of our analysis (Allen 2003). The third component, qI disappears in a time scale from 30 minutes to a day and is attributed to photodamage in PSII (Anon 2018; Murchie and Niyogi 2011; Takahashi and Badger 2011).

The conformational changes induced while NPQ is formed are slower to relax than to be formed. Therefore, NPQ takes more time to relax when the light intensity decreases than it takes time to be formed when the light intensity increase (Kromdijk et al. 2016; Zhu et al. 2004). This shift between the formation and the recovery of NPQ is exacerbated if the plant has already been exposed to fluctuating light intensity and particularly to high light intensity (Demmig-Adams et al. 1999; Kromdijk et al. 2016; Müller et al. 2001; Pérez-Bueno et al. 2008). Therefore, when light intensity is reducing after a period of high light intensity, there is still the presence of NPQ, which means that the sunlight energy which could be used in photochemistry is still released as heat by NPQ. Thus the photosynthesis efficiency is reduced, which reduces the capacity of the plant to assimilate CO_2 resulting in a loss from 12.8 to 30% in carbon fixation (Zhu et al. 2004). This impeded the maximal formation of the yield (Werner et al. 2001). This phenomenon can be worsened in the case of recurrent exposure to excessive sunlight

intensity(Long, Humphries, and Falkowski 1994). Based on these observations, increasing the speed of NPQ relaxation appears as a favourable solution to improve photosynthesis efficiency (Kromdijk et al. 2016; Long et al. 1994). This enhancement of photosynthesis efficiency, by fastening the relaxation kinetics of NPQ, has been shown to increase the yield formation by 15% (Kromdijk et al. 2016).

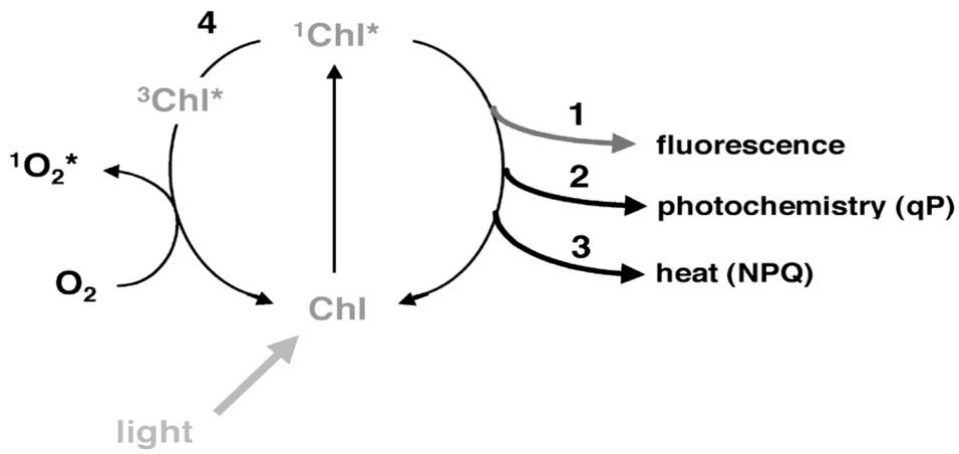

Figure 2: Different ways of dissipation of the chlorophyll excitation. The mechanism of photochemistry which leads to the formation of carbohydrate and the mechanisms of photoprotection, the chlorophyll fluorescence and the heat (NPQ). (Müller, Li, and Niyogi 2001)

Box 1: The Chlorophyll fluorescence parameters used for phenotyping the activity of PSII

Since the 1980s, chlorophyll fluorescence is used as a tool to measure photosynthetic PSII quenching and non-quenching parameters (Schreiber et al. 1995; Ruban 2016). Those kinds of light-addition technic are non-destructive and enable the determination of the fraction of fluorescence quenching that is attributable to photochemical and non-photochemical quenching processes (Bradbury and Baker 1984). The measurement of photosynthetic parameters by the means of chlorophyll fluorescence mostly originates from the assumption that all the PSII RCs are closed by a pulse of saturating light (Schreiber et al. 1995). The fluorescence of PSI is barely used because, in this photosystem, the transfer of energy is done, no matter that the RCs are closed or open (Kramer et al. 2004). The measurement of chlorophyll fluorescence consists first in applying a period of darkness to the plant to open all the RCs (all the Q_A are oxidized). This period of darkness should be long enough to ensure a perfect openness of all the RCs, if it is not the case a pulse of weak FAR-red light should be applied to fully oxidize Q_A. During this period of darkness, the chlorophyll fluorescence is monitored thanks to non-actinic measuring beams, this gives the minimal level of fluorescence F_0 (cf. table 1), the photochemistry is there maximal. Then a saturating is applied (one second or less and an intensity of several thousand µmol m^{-2} s^{-1}) in order to maximally reduce all the Q_A (RCs get closed), the maximal fluorescence level of a dark-adapted leave (F_m) is then observed. During the pulse the quenching is due solely to NPQ (Müller et al. 2001). The difference between F_m and F_0 is termed F_v. The chlorophyll fluorescence can also be monitored on a light-adapted leave enabling the calculation of different photosynthetic parameters. To monitor the chlorophyll fluorescence on a light-adapted leave, a period of actinic light is first applied to the leave and F_p is calculated. If a saturating pulse is applied to this leave the maximum chlorophyll fluorescence yield of the light-adapted leave (F_{mp}) can be calculated. The difference between F_{mp} and F_p is termed F_{qp}. Finally, if a period of darkness is applied on a light-adapted leave the minimum level of chlorophyll fluorescence of the light-adapted leave (F_{0p}) can be obtained (Baker 2008).

Table 1: Chlorophyll fluorescence parameters frequently used to calculate photochemical quenching and non-photochemical quenching parameters .

Parameters	Definition
F, F_p	Fluorescence emission from respectively dark and light-adapted leaves
F_0, F_{0p}	Minimal fluorescence level from respectively dark and light-adapted leaves
F_m , F_{mp}	Maximal fluorescence level from respectively dark and light-adapted leaves
F_v ,F_{vp}	Variable fluorescence level from respectively dark and light-adapted leaves
F_{qp}	Difference in fluorescence level between F_m' and F'
F_{mpp}	Maximal fluorescence level from light adapted leave after a period of darkness

To study the genetics underlying a trait, two sources of variation can be used: natural genetic variation or genetically engineered mutations. In the context of plant improvement, genetic engineering has been frequently used to reveal the genetic and molecular mechanisms underlying the physiology of NPQ (Arber 2010; Jung and Niyogi 2009). By using reverse genetics, researchers created mutants from the model plant *Arabidopsis thaliana* and among those found npq mutants. The *npq1* and *npq2* knockdown mutants were showing defects in the xanthophyll cycle, respectively a deficit in VDE and zeaxanthin epoxidase (Niyogi et al. 2005). The knockdown mutation on the *npq4* gene led to a lack of PsbS protein synthesis (Dall'Osto et al. 2014). All these mutants were presenting a lower NPQ and were more sensitive to light compared to wild-type individuals (WT). While looking at the phenotype of these mutants it has been proven that the genes regulating the xanthophyll cycle and the expression of the PsbS protein were essential in the regulation of NPQ (Niyogi, Grossman, and Björkman 1998; Shikanai et al. 1999). Further, a study conducted on tobacco VPZ mutant lines which were over-expressing violaxanthin de-epoxidase (VDE), zeaxanthin de-epoxidase (ZPE) and PsbS proteins, showed that these lines were presenting an increase of CO_2 uptake and dry matter production under fluctuating light (Kromdijk et al. 2016). Nonetheless, the use of the VPZ construct on *A. thaliana* did not lead to similar results, there was no increase in biomass reported (Garcia-Molina and Leister 2020). Therefore, despite the high number of studies aiming to reveal the genetics underlying NPQ, the genetic regulation of NPQ mechanisms, is still only partially known.

Until now, a large number of discoveries on NPQ regulation have been made by the mean of genetic engineering, however, naturally occurring variation is also used to study NPQ. On earth, plants are growing in various types of environments and under various types of light conditions. Through years of evolution, photosynthesis and the regulatory mechanisms involved in the response to fluctuating light intensity get adapted to each environment begetting natural variation for these traits(Bellan et al. 2020; Demmig-Adams 1998; Johnson et al. 1993). Moreover, the plant genome is composed of three entities of genetic information: the nuclear genome or nucleotype, the mitochondrial genome, and the chloroplast genome. The nuclear genome is bi-parentally inherited and the organelles genomes (plasmotype) are maternally inherited and do not undergo recombination. Even though 99.92 % of the proteins are encoded by the nuclear genome, the chloroplast genome and the plastome play a crucial in the regulation of the respiration and photosynthesis (Budar and Fujii 2012; Greiner and Bock 2013; Joseph et al. 2013; Wang, Tank, and Sang 2000). Therefore, there are important interactions between the nucleotype and the plasmotype in the regulation of photosynthesis and respiration. As non-photochemical quenching is a complex trait whose expression is linked to photosynthesis, its expression is the result of the interaction between nucleotype and plasmotype and the environment (Jung and Niyogi 2009). Therefore, using naturally occurring variation can be a strategy to improve our understanding of the genetic regulation of NPQ.

Box 2: Cytoplasmic swap panel

A cytoplasmic swap panel is a population in which novel nuclear-cytoplasmic combinations are represented. This is possible because in the plant the organelles are maternally inherited while the nuclear genome is bi-parentally inherited. So, by associating the nucleus of one accession with the plasmotype of another accession, new genetic combinations can be created. To establish a cytoplasmic swap panel, the first cross is made between a wild type (WT) individual (nucleotype donor) and a haploid inducer line (cytoplasm donor). In this study, the haploid inducer line used to induce haploidy was the *CENH3-1* GFP-tailswap mutant. This line possesses a variant of the centromere-specific histone protein 3, CENH3 (Britt and Kuppu 2016). The function of the non-mutated protein is the faithful segregation of the chromosomes during the meiosis (Britt and Kuppu 2016). That is why a modification of this protein leads to chromosomes-segregation errors during meiosis or even lethality. Then the nucleotype of the *CENH3-1* mutant is often not transmitted to the progeny. However, despite the mutation, the function of this protein in the *CENH3-1* mutant will remain during the mitosis (Britt and Kuppu 2016). Thus, the progeny is still viable. Therefore, while crossing an accession possessing the CENH3-1 GFP-tailswap mutation as a plasmotype donor with a WT individual as a nucleotype donor, 25-45% of the progeny will be paternal haploid with the plasmotype of the CENH3-1 GFP-tailswap mutated accession(Britt and Kuppu 2016). These offspring are then selfed to obtain a double-haploid homozygous cybrid (Figure 3). The CENH3 mutation has been induced in the accession Col. Therefore, to introduce this mutation in other accessions, individuals of new accessions are crossed as a plasmotype donor with the Col *CENH3-1* mutant as a nucleotype donor (Flood et al. 2020). These crosses work pretty well and give plenty of double-haploid, heterozygote individuals. These individuals are then self-crossed to introduce the mutated gene in both chromosomes, new haploid inducer lines are created (Figure 4).

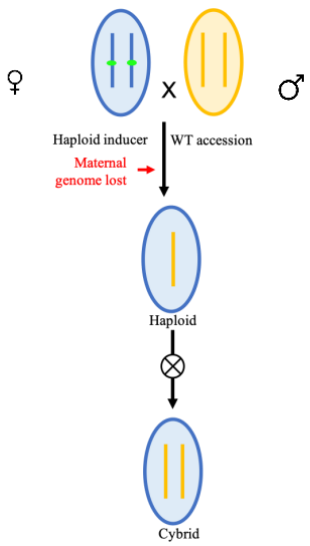

Figure 3:The creation of a cybrid in two generations by crossing a haploid inducer as a nucleotype donor and a WT individual as a plasmotype donor, and by sefling the progeny.

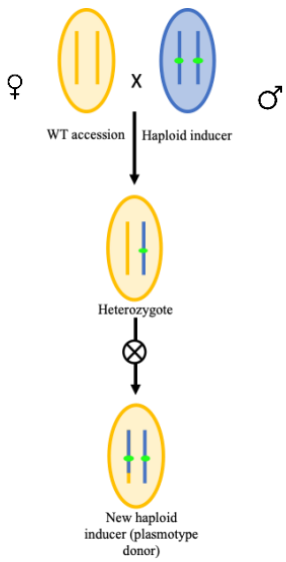

Figure 4: The creation of a new haploid inducer from a cross between a WT individual as a plasmotype donor and a Col CENH3 mutant line as a nucleotype donor.

The widespread crucifer, *A. thaliana* has been established as the plant model to study the genetics underlying complex traits. The adaptation of *A. thaliana* genome to various types of ecosystems, by the fixation of beneficial mutations, provides considerable natural genetic variations among the different accessions of this species. Moreover, *A. thaliana* possesses only 5 chromosomes and is a selfer which can be out-crossed (Alonso-Blanco and Koornneef 2000; Jung and Niyogi 2009; Meinke et al. 1998), these are assets for the establishment of segregating populations.

The naturally occurring variation of *A. thaliana* has been used by Flood et al. (2020) to create a cytoplasmic swap (Box 2). Thanks to this population the impact on the phenotype of novel plasmotypes and nucleotypes associations was assessed. On this cytoplasmic swap panel, many photosynthetic-related parameters including non-photochemical quenching (NPQ, qE, and qI) and quantum efficiency for photosynthetic parameters (ϕPSII, ϕNO, ϕNPQ) have been measured (Appendix 1). These parameters were measured under steady and fluctuating light. The fluctuating light environment is essential to express NPQ and measure its variations because it reproduces the natural growing conditions of the plants. For this experiment, a fluorometer named Dynamic Environmental Photosynthesis Imager (DEPI) has been used. This experimental platform generates fluctuating light and provides high-throughput measurements of photosynthetic parameters such as ϕPSII, NPQ, qE, and qI (Cruz et al. 2016).

By phenotyping the cybrids panel under fluctuating light, two important results arose. First, the outcomes of the measurements of the ϕPSII under fluctuating light showed that Ely plasmotype combined with any nucleotype was showing a lower ϕPSII compared to the other cybrids of the panel (Figure 5A). Previously the origin of this lower ϕPSII has been found to originate from a mutation happening in the psbA gene located in Ely chloroplast (El-Lithy et al. 2005). The mutation of this gene results in the alteration of D1 protein which greatly reduces ϕPSII but provides to the plant resistance against pesticides made from atrazine (El-Lithy et al. 2005). Thus, the low ϕPSII observed in the cybrids containing Ely plasmotype in Flood et al. (2020) panel, was due to the *psbA* mutation in the chloroplast. Then, the results of NPQ phenotypic variations revealed that Ely nucleotype associated with any other plasmotype was showing a higher NPQ compared to the other cybrids (Figure 5B) (Flood et al. 2020). This higher NPQ phenotype of the Ely nucleus has been further linked with a higher qE.

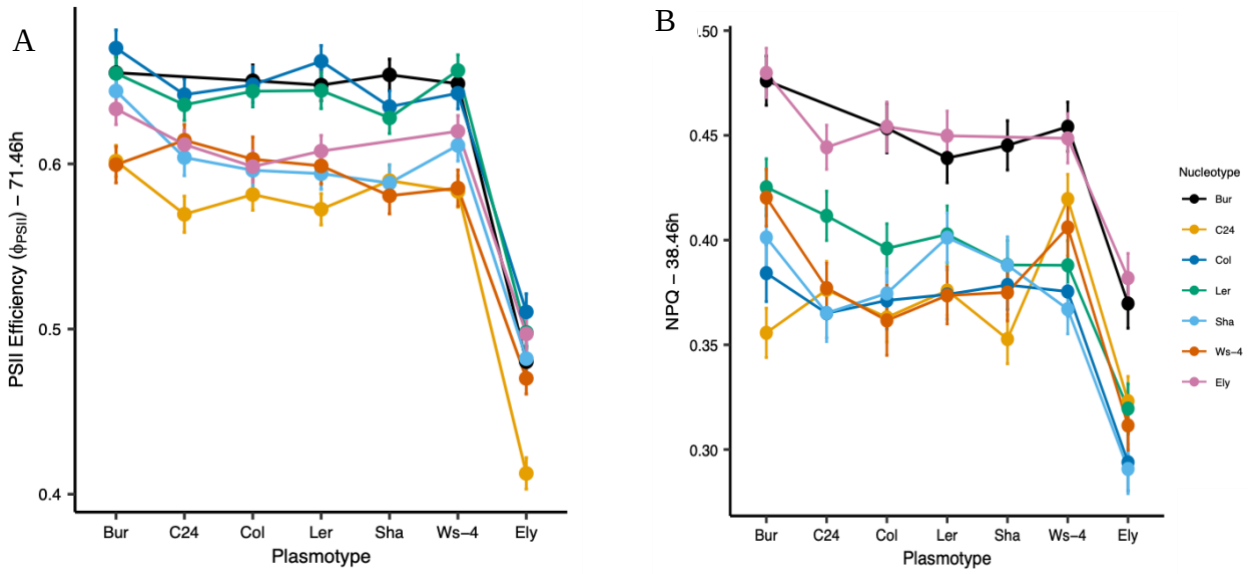

Figure 5: (A) The ϕPSII is always lower when Ely plasmotype (represented on the right side of the X axis) is associated with any other nucleus. (B) On the contrary, when Ely nucleus represented by the pink line is associated with any other plasmotype and measured under fluctuating light then NPQ is higher than for the other cybrids, except those containing Bur nucleus (Flood et al. 2020).

The results found by El-Lithy et al., on the *psbA* mutation occurring in Ely has been used by Flood et al. in 2016. Their study aimed to demonstrate that in self-fertilizing organisms, the strong selection on beneficial organellar mutations, can lead to nuclear genome hitchhiking with these organellar genomes. This, to the point, that the emergence of a beneficial mutation in the organelles can reduce diversity. After studying the repartition of the atrazine resistant phenotype in England, the conclusion of their work was that all the atrazine resistant accessions were having the same nuclear backgrounds. The nuclear genome hitchhiked with the *psbA* mutation located in the chloroplast genome (Flood et al. 2016). However, after this conclusion has been established, another atrazine resistant genotype, Hunley (Hun), has been discovered on the collection of accessions picked up on the English railway (Mark Aarts personal communication). After genotyping the Hun nucleus for the 39 nuclear SNPs used to genotype the atrazine resistant individuals, it has been shown that its nuclear genome was different from the other atrazine resistant accessions. Later, the genotyping of its chloroplast genome shown that, like Ely, Hun was presenting the *psbA* mutation. These results demonstrate that Hun and Ely, both atrazine resistant accessions, might have evolved independently.

Altogether these results show two important facts, the mechanism of NPQ was differently regulated by the nucleus of the Ely accession (Flood et al. 2020), while ϕPSII was significantly lower in this accession (El-Lithy et al. 2005). Then, several questions emerged from these results. First, it remains unknown if the Ely nucleus evolved to compensate for the low ϕPSII resulting from the *psbA* mutation occurring in the chloroplast of this accession, or if the nuclear variation of Ely was present before the *psbA* mutation arose. In Ely, the *psbA* mutation leads to a lower ϕPSII, while the nuclear genome is compensating this low ϕPSII by

increasing NPQ. None of these measurements have been done yet for Hun, the NPQ phenotype of Hun nucleus remains unknown. Therefore, in this project three cybrids Hun_{Col}, Ely_{Col}, Col_{Col} were used. The NPQ phenotype of Hun_{Col} was compared with the NPQ phenotype of Ely_{Col}. As the plasmotype was the same in both cybrids, the impact of each nucleus on the NPQ phenotype could be analysed with more precision. The presence or absence of the same NPQ phenotype from Hun nucleus and Ely nucleus will give us insight into the type of evolution of Ely nucleus.

Moreover, recent research was undertaken in the Laboratory of Genetics at Wageningen University and Research and established that the rate of the qE component was significantly higher in Ely accession compared to the panel's average. Hence, two other questions emerge. Is the rate of NPQ more flexible when regulated by the Ely nucleus? Precisely, due to its higher level of qE will Ely NPQ relax faster compared to the NPQ regulated by the nucleus of any other accession, or will Ely nucleus always produce a higher NPQ? An improved plasticity of NPQ will probably confer advantages to the plant under fluctuating light. While a higher NPQ leads to a reduction of ϕCO2 and eventually to a reduction in yield (Murchie and Niyogi 2011). To investigate these questions, it will be relevant to explore the genetic and physiological proprieties underlying the NPQ phenotype of the Ely nucleus.

The major aim of this thesis was to investigate further the discovery previously made by Flood et al. 2020, concerning the difference in NPQ's regulation of the Ely nucleus. The work was then be divided into two parts. First, a fluctuating light response curve was undertaken to compare the NPQ phenotypic variation of Hun and Ely nucleus and establish the variation of the different photosynthetic parameters (ϕPSII, NPQ, qE, qI, ϕNO, ϕNPQ) (Appendix 1) under fluctuating light intensity. The phenotypic results of Hun were also compared with those of Ely to get insight into the origin of Ely nucleus variation. Secondly, an NPQ transient relaxation experiment was carried out to assess whether a higher rate of qE can lead to a faster relaxation of NPQ.

2 Material and methods

2.1 Plant material

2.1.1 Growing conditions

The plant material for the phenotypic experiments is generated from *A. thaliana* seeds. The seeds of the different *A. thaliana* accessions were sown in Petri dishes on soaked filter paper with 0.6 mL of Milli-Q water for small Petri dishes or 1 mL for big Petri dishes. Then the seeds were placed in a cold room (4°C) for one week to induce vernalisation (cold period necessary for germination). Then, these plants were placed in a climate room (24°C with a rhythm of 16/8h day/night) for 24h to induce germination. The germinates seeds were sown on pre-soaked Rockwool in a climate chamber. In this chamber the light was on for 16h hours during the days at 200 $\mu molm^{-2}s^{-1}$ photon irradiances, the temperature was 20°C during the day and 18°C during the night, the relative humidity was 70%. The seedlings were watered 3 times a week with the Hyponex growth mix. At two weeks after sowing, the best-looking seedlings were collected to be measured.

2.1.2 The cytoplasmic swap panels

The phenotyped population was a cytoplasmic swap panel made from three *A. thaliana* accessions: Ely, Hun, and Col. The crosses have been made before this thesis work. The accession Col for which *CENH3-1 GFP-tailswap* mutation exists has been used as a plasmotype donor. Col *CENH3-1* mutant has been crossed with Ely Hun and Col WT as nucleotype donors. The crosses Col *CENH3-1* mutant*Col WT served as a control. The haploid offspring of these three crosses have then been sefled to obtain homozygous cybrids. The cybrids resulting from the cross Ely WT* Col *CENH3-1* mutant contained the nucleotype of Ely and the plasmotype of Col and were noted Ely_{Col}. The cybrids resulting from the cross Hun WT* Col *CENH3-1* mutant contained the nucleotype of Hun and the plasmotype of Col and were noted Hun_{Col}. The cybrid resulting from the cross Col WT* Col *CENH3-1* mutant contained the nucleotype of Col and the plasmotype of Col and were noted Col_{Col} (Appendix 4).

2.2 PSI PlantScreen Module

The PSI PlantScreen Module (Photon Systems Instruments, Czech Republic) is a phenotyping platform. Four types of cameras are integrated into this platform: FC cameras for chlorophyll fluorescence measurement, RGB1 (pictures from the top), and RGB2 (picture from the side) cameras are used to take measurements of the plants and 3D camera use to make 3D measurements of the plant. In this project only, the FC cameras will be used. Four software packages were used. The PlantScreen server which is the main machine control server, the Fluorcam (explained in 2.3), the PlantScreen Scheduler (version 1.6.1) which is used to program experiments, and the PlantdataAnalyzer (version 3.1.6.19) which is used to extract data. The PlantScreen software can be used through two different modes all cameras and only

FC. These modes can be switched thanks to a fifth software, the PlantScreen configuration Switcher. The light response curve has been performed under the Only FC mode which permits to perform several protocols on the same tray consecutively without handling. On the contrary, the NPQ transient relaxation curve has been performed under all camera mode. Under this mode, the tray goes out at the end of each experiment and the next experiment needs to be set up manually.

2.3 Fluorcam

The Fluorcam is a kinetic imaging fluorometer developed by Photon Systems Instruments. It contains a camera (FC camera cf. 2.2) with modules to capture and grab images, and modules to control the flashes, actinic light, and saturating flashes that are generated by version-dependent light sources. The Fluorcam software is used to design a protocol to capture fluorescence transients. The protocol consists of a list of instructions specifying when and which actions the Fluorcam instrument has to perform.

- *FPperiod = 200s* : determines the length of a period
- *FP / Fmp= FP + FPperiod* : determines the frame of the period
- *<FP, FP + FPmeasurement .. FPperiod>=>mfmsub*: determines the sequence of measurement during one period
- *<FP>=> SI_Act2 ()*: determines the intensity of the actinic light, the intensity should be added between the brackets, the intensity is not in uE but %, a conversion curve has been established using a chlorophyllmeter (Appendix 2).
- *<FP>=>act2(FPperiod)*: determines the length of the period during which the actinic light should be on.
- *<Fmp>=> Satpulse()*: induces a saturating pulse for a certain period length which is determined between brackets
- *<Fmp>=>mpulse*: induces measurement during the saturating pulse
- *<FARstart>=>FAR(FRPeriod)* induces FAR red light for a certain period determined between brackets.

The protocol written in the Fluorcam software was saved to a database linked to the PlantScreen Scheduler software.

2.4 Phenotyping

2.4.1 The fluctuating light response curve

2.4.1.1 Fluctuating light response curve experiment

The light response curve experiment was performed through the PSI PlantScreen Module Platform through the FC mode. The protocol was started thanks to the PSI PlantScreen Module. The seedlings were transported from the climate chamber to the PSI PlantScreen

Module in a transparent genetic transport box. The seedlings were placed in a tray containing twenty emplacements, thus, twenty plants were phenotyped at a time. One tray with twenty seedlings corresponded to one batch. This experiment was done twice, each time the batch was composed of six Hun_{Col}, six Col_{Col}, and seven Ely_{Col} (Appendix 7). As one round of measurements was lasting seven hours, only one round a day was performed to keep the measurement as homogenous as possible. All the rounds were started at 10 a. m.

2.4.1.2 Design

The design of the fluctuating light response curve experiment was divided into two protocols.

The first protocol was an F_v/F_m protocol, the purpose of this experiment was to obtain the value of F_m and F_v essential for the calculation of the photosynthetic parameters (cf. formulas Appendix). The protocol was preceded by thirty minutes of dark adaptation. Right after the thirty minutes of darkness, the F_v/F_m protocol was starting with the extension of the darkness period for twenty seconds. During this time length, one measurement was performed every second. The average of these measurements was used to get F_0. Then a saturating pulse was applied for height-hundred milliseconds (ms), during which six measurements were performed. The average of the six measurements was used to calculate F_m. F_v was obtained by making the difference between F_m and F_0. This protocol was done only one time, at the beginning of the experiment (Figure 22.A Appendix 3).

The second protocol of the experiment was the core protocol used to fluctuate light intensity and express the NPQ phenotype. This core protocol consisted of the repetition of a protocol twenty-four times. The protocol started with the application of fixed actinic light intensity for sixteen minutes. The time length of this period had to be long enough to obtain a stable F_p (no variation of the fluorescence level). At the end of this period of actinic light, a saturating pulse was applied with the actinic light still on. This saturating pulse was applied for height hundred ms and six measurements were performed during this pulse. The average of these measurements was used to obtain the value of F_{mp}. After that, the actinic light was let on for fifty-height seconds to come back to a stable F_p. Then the light was switched off, and after three seconds FAR red light was applied for one second to fully oxidize the Q_A sites. After that, a relaxation period of one-hundred twenty seconds in the dark was completed during which measurements were performed every ten seconds. The average of these measurements was used to measure F_{0p}. At the end of this period of dark relaxation, a third saturating pulse was applied for height-hundred ms and six measurements were done during this pulse. The average of the measurement of this pulse was used to obtain F_{mpp} (Figure 22.B Appendix 3).

This protocol was performed for different actinic light intensities 65, 131, 129, 259, 191, 383, 250, 500, 304, 605, 354, 707, 397, 793, 433, 866, 462, 924, 483, 966, 496, 991, 500, 1000, µmol. m^{-2}. s^{-1}. So, for the first repetition of the protocol, the actinic light intensity was 65 µmol. m^{-2}. s^{-1}, for the second repetition of the protocol the actinic light intensity applied, was 131

μmol. m^{-2}. s^{-1}, and this until 1000 μmol. m^{-2}. s^{-1}. The twenty-six protocols were implemented consecutively, giving a global protocol of seven hours. The application of these different light intensities consisted of expressing the NPQ phenotype. From the measurement carried out during this experiment, NPQ, ϕPSII, qE, qI, NPQt, ϕNO, ϕNPQ were calculated.

2.4.1.3 The use of NPQ(t) instead of NPQ

The total duration of the fluctuating light response curve was seven hours. During this time, photodamage (qI) will accumulate into the chloroplast, leaves movements and chloroplast movements will occur. The calculation of F_m and F_{mp} depends on the level of fluorescence emitted by PSII. This level is contingent with the leaves' surface presents under the camera when the measurement is taken and with the chloroplasts position and qI amount at the moment of the measurement. As these elements will not stay stable for seven hours, then, the measurement of PSII fluorescence will also fluctuate. Thus, F_m measurement taken only once at the beginning of the experiment would not always overlap with the measurement of F_{mp}. NPQ(t) is an adjusted version of NPQ as it is not calculated from F_m (Appendix 1). Discarding F_m from the calculation is a method used to correct for leaves movements, chloroplast movements, and qI accumulation. Therefore, the calculation of NPQ(t) was used to study the phenotypic variations of NPQ. Via the same principle ϕNO(t), and ϕNPQ(t) were also calculated and used instead of ϕNO and ϕNPQ (Appendix 1). However, qE and qI were not estimated from qE(t) and qI(t) because the measurement realised during the program did not include F_{0pp} essential for the calculation of qE(t) and qI(t).

2.4.2 NPQ transient relaxation

2.4.2.1 NPQ transient relaxation experiment

The NPQ relaxation was monitored in the PSI PlantScreen Module through the all cameras mode. The protocol was started thanks to the PSI PlantScreen Module. The protocol was repeated six times, with as only difference the starting moment of the first saturating pulse of relaxation period (50 μmol. m^{-2}. s^{-1}) sifted from five seconds compared to the previous protocol. For this experiment, the seedlings were transported from the climate room to the PSI PlantScreen Module in a transparent genetic transport box. The seedlings were placed in a tray containing twenty emplacements, thus, twenty plants were phenotyped at a time. The tray used to carry out this experiment contained ten Ely_{Col} and ten Col_{Col}. These twenty seedlings were constituting one batch (Appendix 7). The measurement of one batch was lasting twenty minutes, therefore all the batches have been measured in one day. The first measurement started at 10 a.m. and the last one at 5:30 p.m.

2.4.2.2 NPQ transient relaxation design

The NPQ relaxation experiment consisted of only one protocol composed of three parts. First of all, a dark adaption period of thirty minutes was applied to the plant. Then, as for the

fluctuating light response curve, an F_v/F_m protocol was applied to obtain Fm essential for the calculation of NPQ. At the beginning of the F_v/F_m protocol, the period of darkness was continued for twenty seconds during which the measurement of F_0 was performed by doing one measurement every second. Right after this period of dark, a first saturating pulse was applied for height hundred ms, six measurements were taken during this pulse. From this saturating pulse, F_m was calculated by doing the average of the six measurements. Then, the seedlings were exposed alternatively to 1000, 100, 1000, 100, 1000 μmol. m^{-2}. s^{-1}, each light intensity was applied for three minutes. The application of these different light intensities to the plants was used to reproduce fluctuating light and express the NPQ phenotype. The third part of this protocol was the monitoring of the NPQ relaxation under 50 μmol. m^{-2}. s^{-1} for five minutes. Small light intensity was kept because the epoxidation of zeaxanthin to violaxanthin is light-dependent. Directly after the actinic light fluctuation was stopped, actinic light of 50 μmol. m^{-2}. s^{-1} was turned on and a saturating pulse was applied every thirty seconds for five minutes. Again, six measurements were carried out during each saturating pulse and the average of these measurements was used to calculate F_{mp} which was used to calculate NPQ (Figure 23 Appendix 3).

The experiment was repeated in six batches. For each new batch, the protocol was adapted in a way that the first saturating pulse of the 50 μmol. m^{-2}. s^{-1} relaxation period was sifted of five seconds compared to the previous batch. Thus, for batch number 1, the first saturating pulse in the actinic light relaxation period was applied zero seconds after the actinic light at 50 μmol. m^{-2}. s^{-1} was turned on, while for batch number 2, the first saturating pulse was applied five seconds after the actinic light at 50 μmol. m^{-2}. s^{-1} was turned on. This sifting step was repeated up to thirty seconds. Thus, for each batch, measurements were taken every thirty seconds but by combining the results of each batch, the values of NPQ relaxation were only spaced of five seconds. Then, by combining the values of the batches the relaxation of NPQ was monitored for five minutes with intervals of five seconds between each value of NPQ. On a timescale of zero seconds to three-hundred twenty-five seconds, one measurement was done every five seconds so in total sixty-five measurements were done. This set up aimed to have the most measurements possible, without having for one batch a saturating pulse applied every five seconds. Too close measurements will have kept the Q_A reduced and not have been accurate to measure the relaxation of NPQ.

In total each round last fifteen minutes, so in this experiment, the value of F_m was still accurate at the end of the experiment. Therefore, we kept the NPQ formula to visualize the relaxation of the NPQ phenotype.

2.5 Statistics

The statistics were performed under Rstudio the packages used were: reshape, ggplot2, lme4, lmerTest, dplyr, and TiddyR.

For the fluctuating light response curve, the analyses of the quenching and non-quenching parameters were performed as follows. The value of each parameter was calculated

per time point and cybrid by averaging the value from the individuals of the two batches. For that, a linear mixed model was performed per cybrid and per time point to obtain the adjusted means which were representing the value of the parameter. The linear mixed model was used here to correct for the batch effect. This test was followed by a one-way ANOVA, performed per cybrid and per time point. The one-way ANOVA was used to verify whether the cybrids were a source of variation of the quenching and non-quenching parameters. Before performing the ANOVA, the assumptions have been checked and the risk α was set up at 5%. After the ANOVA, a posthoc test with a Tukey p-value was performed to establishes if the impact of the cybrids on the quenching and non-quenching parameters were significantly different from the others. As multiple groups were compared the Tukey p-value was adjusted for the number of comparisons between groups.

For the NPQ relaxation curve, a one-way ANOVA was performed per time point with the cybrid (Ely_{Col}, Col_{Col}) as a factor and the NPQ variation and ϕPSII variation as the response variable α was set up at 5%.

3 Results

During this thesis, two phenotyping experiments were conducted, a fluctuating light response curve and then an NPQ relaxation curve. Both of these experiments were carried out on cybrids. Hun_{Col}, Ely_{Col}, and Col_{Col} were used for the fluctuating light response curve while Ely_{Col} and Col_{Col} were used for the NPQ relaxation. The phenotypic platform PSI PlantScreen Module was used to make the measurements. In this part, the main results of the two phenotyping experiments will be presented. The results not given here are available in the Appendix.

3.1 The fluctuating light response curve

The fluctuating light response curve aimed to fluctuate the light intensity to reveal the NPQ phenotype(s). This experiment was designed to mimic the variation of the light occurring during the day due to clouds passing in front of the sun and leaves movements. To reproduce these variations, a pattern was created: a period of low actinic light intensity was followed by a period of high actinic light intensity, then the light intensity was fluctuating (Figure 6). The outcome of this experiment showed the phenotypic variations of NPQ, of the photosynthetic parameters (ϕPSII, ϕNO, ϕNPQ), and the sub-mechanisms of NPQ (qE and qI). The phenotypic variations of all these parameters could then be compared with each other and between cybrids. In this part, the variations of the quenching and non-quenching parameters were plotted against the time while their variations were measured through the fluctuation of the light intensity. This was possible thanks to a correspondence established between the time and the light intensity (Figure 6) (Appendix 2). This plotting method allowed the visualization of the concatenation of light intensities and a more accurate analysis of the effect of fluctuating light on the quenching and non-quenching parameters' phenotypes. Thus, per time point the phenotypic value of each parameter was given per cybrid and was corresponding to the phenotypic value of the parameter for each cybrid per light intensity.

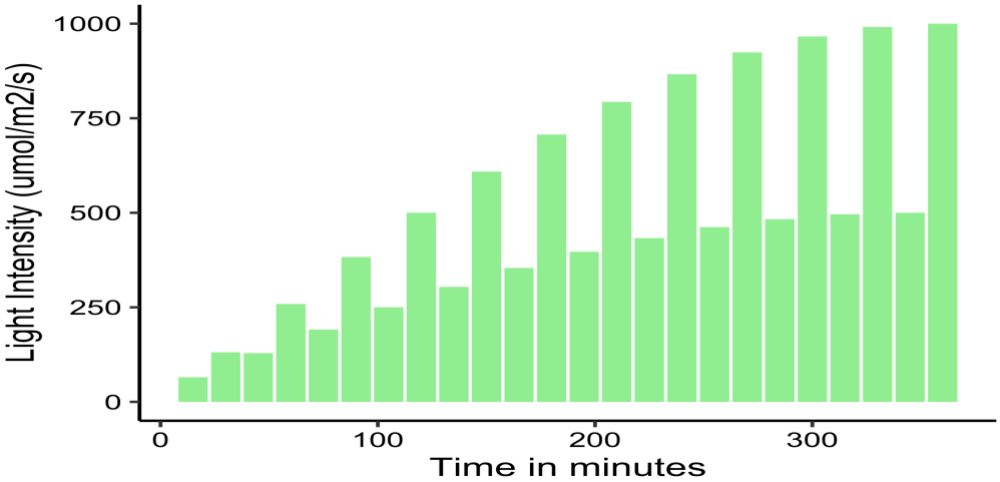

Figure 6:The entire second protocol of the fluctuating light response curve experiment is represented here. The Fv/Fm protocol is not shown. On the Y-axis the actinic light intensity (µmol. m-2. s-1) is represented, the height of each bar represents the actinic light intensity used in one protocol. On the X-axis, the time is represented, the weight of a bar represents the time length of one protocol so fifteen minutes for each bar. The first bar represents the first protocol with an actinic light intensity of 65 µmol. m-2. s-1 and a time length of fifteen minutes.

3.1.1 NPQ(t) phenotypes

Results anterior to this thesis have established that, under fluctuating light intensity, NPQ was upregulated by Ely nucleus while this has not been measured yet for Hun nucleus. Therefore, our first interest was to compare Ely_{Col} and Hun_{Col} NPQ phenotypes, after the fluctuation of the light intensity. As the fluctuating light response curve lasted seven hours, NPQ(t) was used instead of NPQ. The results of our experiment are shown in figure 7, the phenotypic variations of NPQ(t) are represented for the twenty-four light-intensities and for each cybrid. For all the cybrids NPQ(t) was increasing when the light intensity increased. The cybrid Ely_{Col} was showing a higher NPQ(t) compared to Col_{Col} and Hun_{Col}, and this difference was increased at higher light intensities (Figure 7). On the contrary, Hun_{Col} was showing the lower NPQ(t) (Figure 7). The results of the posthoc test were that the difference in NPQ(t) between Ely_{Col} and Hun_{Col} and Col_{Col} was almost always significant before one-hundred-fifty minutes corresponding to 605 µmol. m^{-2}. s^{-1} and always significant after this time for the periods of high and low light intensities (Figure 8). Thus, above 605 µmol. m^{-2}. s^{-1} Ely_{Col} has always a significantly higher NPQ(t) compared to Col_{Col} and Hun_{Col}. The difference in NPQ(t) between Col_{Col} and Hun_{Col} was mostly significant for the periods of high light intensities only (Figure 8).

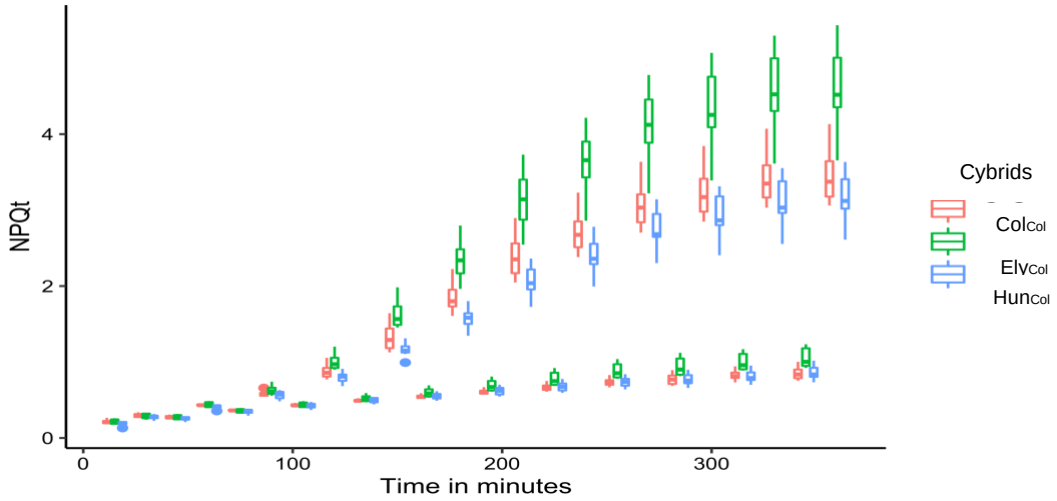

Figure 7: NPQ(t) increases with the increase of actinic light intensity. The boxes represent the distribution of the NPQ(t) values of the fourteen Ely$_{Col}$, Col$_{Col}$, and the twelve Hun$_{Col}$ per light intensity. The lower extremity of the line represents the minimal value, the higher extremity of the line represents the maximal value. The first rectangle represents the first quartile, the second rectangle the third quartile. The line in the middle of the rectangles is the median and corresponds to the middle value of the fourteen or twelve individuals. Within the first and third quartile, 50% of the values are contained. The first group of boxes on the left represents the values of NPQ(t) when the actinic light intensity was 65 µmol. m^{-2}. s^{-1} and this pattern goes on until the last group of boxes which represents the values of NPQ(t) when the actinic light intensity was 1000 µmol. m^{-2}. s^{-1}.

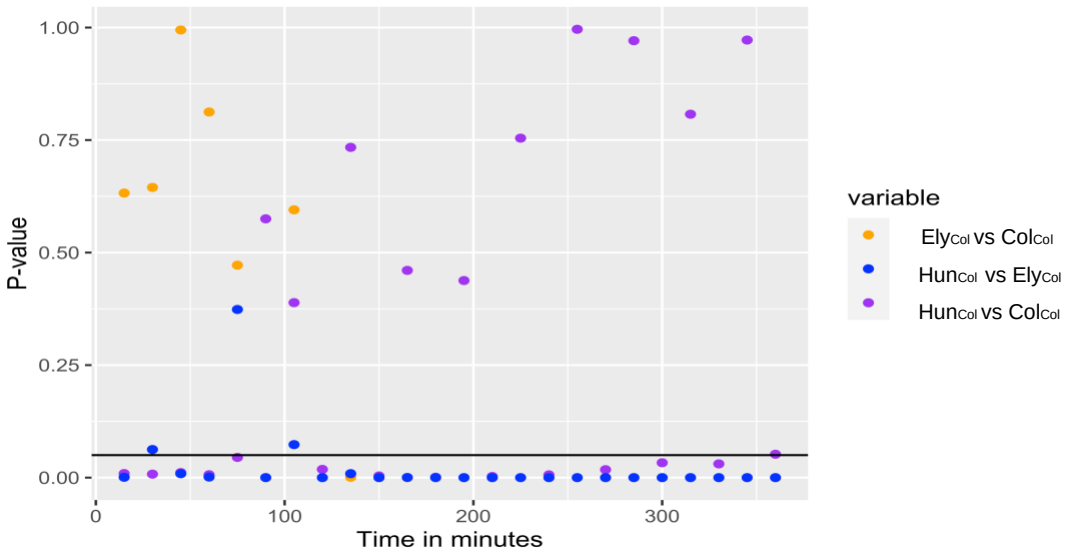

Figure 8: The results of the posthoc test for the variations of NPQ(t) between the cybrids, with a Tukey p-value adjustment, are represented here. The black line represents the risk α fixed here at 0.05. The dots represent the adjusted Tukey p-value obtained from the posthoc test. Each column of dots represents the results of one posthoc test for the three cybrids, per time point so per light intensity. The first column on the left corresponds to the result of the posthoc test when the actinic light intensity is 65 µmol. m^{-2}. s^{-1} and this pattern continues until 1000 µmol. m^{-2}. s^{-1}.

3.1.2 NPQ(t) vs ϕPSII

By the previous results, we have demonstrated, that NPQ(t) was higher in Ely_{Col} than Col_{Col} and Hun_{Col}. In this experiment, all the cybrids contain Col plasmotype and thus do not contain the *psbA* mutation responsible for a low ϕPSII. Thus, ϕPSII is supposed to be constant among the cybrids. Therefore, the impact of each nucleus on NPQ(t) can be studied independently of ϕPSII variations. For that, the variations of the ratio ϕPSII/NPQ(t) were compared among the three cybrids, through the fluctuation of the light intensity (Figure 9A). As the plasmotype is the same in all the cybrids the variations of the ratio should be uniquely due to the variations of NPQ(t). We noticed that the NPQ(t) phenotype is most pronounced under high light intensities and that the relation between NPQ(t) and ϕPSII is there linear (Figure 9A). Thus, we selected a subset of the highest light intensities (605, 707, 793, 866, 924, 96, 991, µmol. m^{-2}. s^{-1}) for which we studied the variations of the ratio ϕPSII/NPQ(t) (Figure 9B). Then, for each cybrid, a linear equation was obtained for ϕPSII/NPQ(t). The slopes represent the variation of the ratio ϕPSII/NPQ(t) through the decrease of light intensity. The intercepts represent the value of NPQ(t) when ϕPSII was equal to 0. However, this value is theoretical because ϕPSII cannot be equal to 0. Two important results arose from this experiment. Firstly, three distinct slopes and intercepts were obtained (Figure 9B). Moreover, when the light intensity increases (going to the left side of figure 9B), for the same level of ϕPSII Ely_{Col} has more NPQ(t) compared to Col_{Col} and Hun_{Col}. Then, the posthoc test showed that the differences between intercepts were all significant like seen with the values of the slopes (Tables 1 and 2).

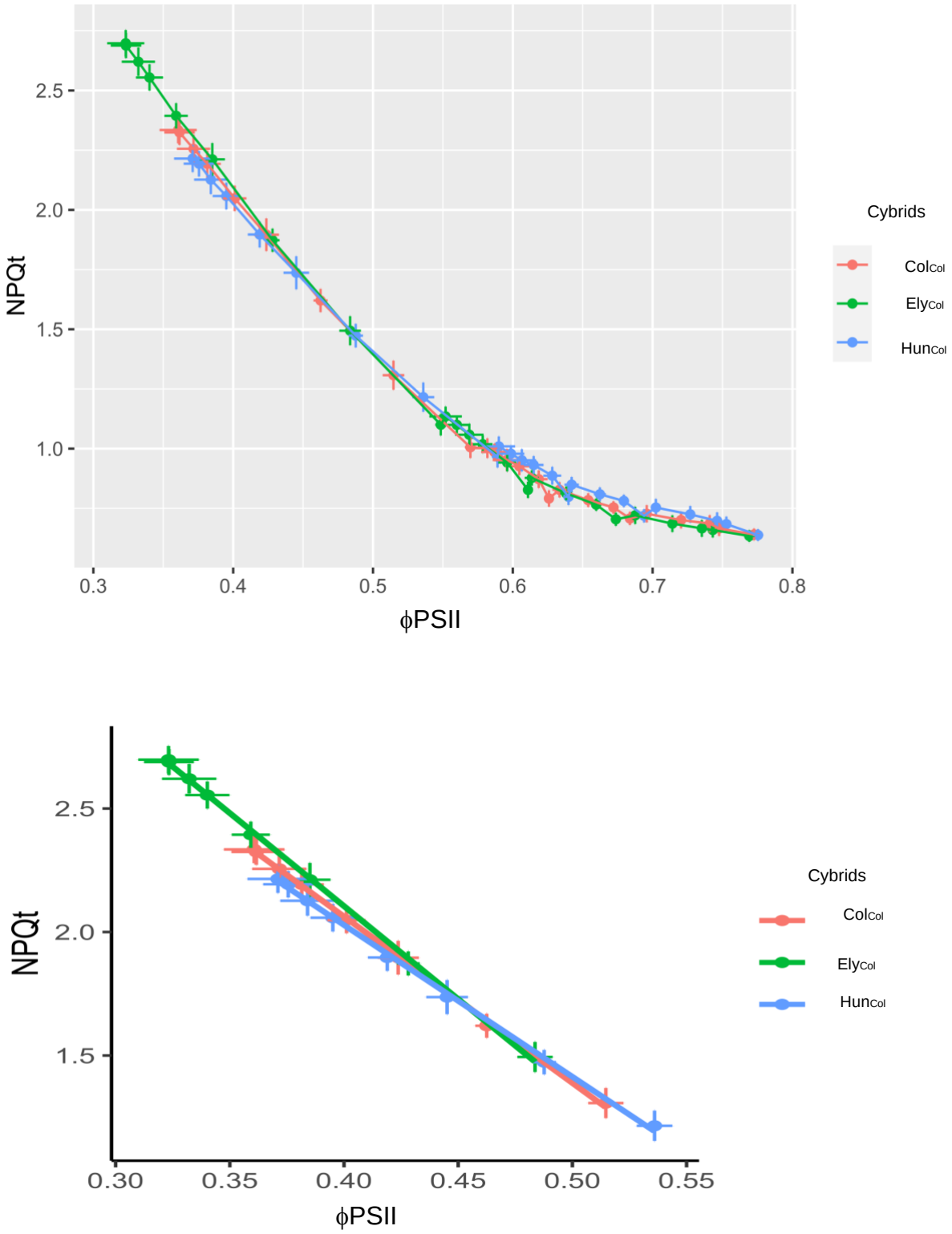

Figure 9: (A) The variations of the ratio ϕPSII/ NPQt for the twenty-four light intensities. (B) The variations of the ratio ϕPSII/ NPQt for a subset of high light intensities 605, 707, 793, 866, 924, 96, 991, 1000 µmol.m-2.s-1. On the left side of the figure, the highest light intensities of the subset are represented, on the right side of the figure the lowest light intensities of the subset are represented. For all the cybrids NPQ(t) and ϕPSII are negatively correlated when ϕPSII increases (with the decrease of the light intensity) NPQ(t) decreases, and reversibly.

Contrast	p-value
Col_{Col} – Ely_{Col}	<0.0001
Col_{Col} – Hun_{Col}	<0.0001
Ely_{Col} – Hun_{Col}	<0.0001

Table 1: The results of the posthoc test with the adjusted Tukey p-value for the slopes of the equations of the figure presented in figure 9.

Contrast	p-value
Col_{Col} – Ely_{Col}	<0.0001
Col_{Col} – Hun_{Col}	0.0001
Ely_{Col} – Hun_{Col}	<0.0001

Table 2: The results of the posthoc test with the adjusted Tukey p-value for the intercept of the equations of the figure presented in figure 9.

3.1.3 ϕNO(t) and ϕNPQ(t) at high light intensities.

As NPQ is calculated from the ratio of ϕNO over ϕNPQ, a difference in NPQ, must mean a difference in this ratio. For the same reasons as we used NPQ(t), we used here ϕNO(t) and ϕNPQ(t). To understand the origin(s) of upregulation of NPQ(t) seen for Ely_{Col} the variations of ϕNO(t) and ϕNPQ(t) were independently studied for the subset of high light intensities used to study ϕPSII/NPQ(t). The upregulation of NPQ(t) seen in Ely_{Col} could be explained by a downregulation of ϕNO(t) or an upregulation of ϕNPQ(t) compared to ϕNO(t) and ϕNPQ(t) in Col_{Col} and Hun_{Col}.

The individual variations of ϕNO(t), known as the sum of non-regulated heat-dissipation and fluorescence emission, show that ϕNO(t) decreases when the light intensity increase (Figure 10). Ely_{Col} ϕNO(t) started at a lower value and is faster to decrease than ϕNO(t) of Hun_{Col} and Col_{Col}. Hun_{Col} presents the slowest decrease of ϕNO(t) (Figure 10). The result of the posthoc test is that for this subset of high light intensities the decrease of ϕNO(t) in Ely_{Col} is significantly faster than the decrease of ϕNO(t) in Hun_{Col} and Col_{Col} (Figure 11). For Hun_{Col} the decrease of ϕNO(t) is significantly slower than the decrease of ϕNO(t) for Ely_{Col} and Col_{Col} except for the 605 μmol. m^{-2}. s^{-1}.

After, studying the individual variation of ϕNO(t), we studied the individual variations of the other part of the ratio: ϕNPQ(t). ϕNPQ(t) is known as the regulated thermal energy dissipation linked to NPQ. The variations of ϕNPQ(t) for the subset of high light intensities show that ϕNPQ(t) increases regardless of the cybrid (Figure 12). The increase of ϕNPQ(t) is faster in Ely_{Col} compared to Col_{Col} and Hun_{Col} (Figure 12). On the contrary, Hun_{Col} shows the slowest ϕNPQ(t) (Figure 12). The results of the posthoc test are that, at high light intensities,

ϕNPQ(t) increases significantly faster in Ely_{Col} compared to ϕNPQ(t) in Col_{Col} and Hun_{Col} (Figure 13). For Hun_{Col} the increase of ϕNPQ(t) is significantly slower than the increase of ϕNPQ(t) for the two other cybrids (Figure 13).

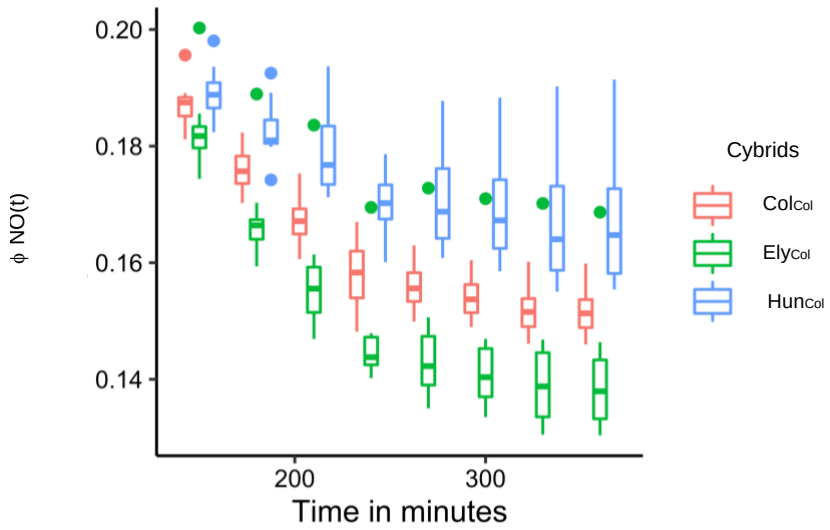

Figure 10: The variations of ϕNO(t) for the subset of high light intensities, 605, 707, 793, 866, 924, 96, 991, 1000 µmol. m-2. s-1. When the light intensity increases ϕNO(t) decreases. The boxes of this figure can be read as the boxes of figure 7. The first group of boxes on the left represent the values of ϕNO(t) per cybrids when the actinic light intensity was 605 µmol. m-2. s-1, and this until 1000 µmol. m-2. s-1.

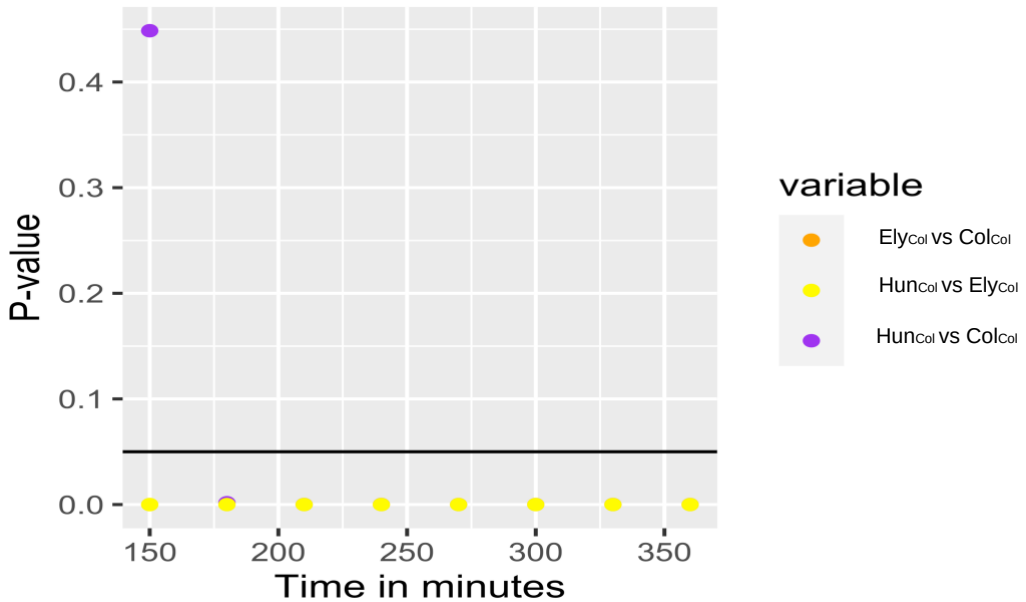

Figure 11: This figure represents the results of the posthoc test with the adjusted Tukey p-value for the variations of ϕNO(t) for the subset of high light intensities and between the cybrids. The black line represents the risk α fixed here at 0.05. The dots represent the adjusted Tukey p-value obtained from the posthoc test. Each column of dots represents one posthoc test for the

three cybrids, per time point so per light intensity. The first column on the left corresponds to the results of the posthoc test when the light intensity is 605 µmol. m-2. s-1, and then this pattern continues until 1000 µmol. m-2. s-1.

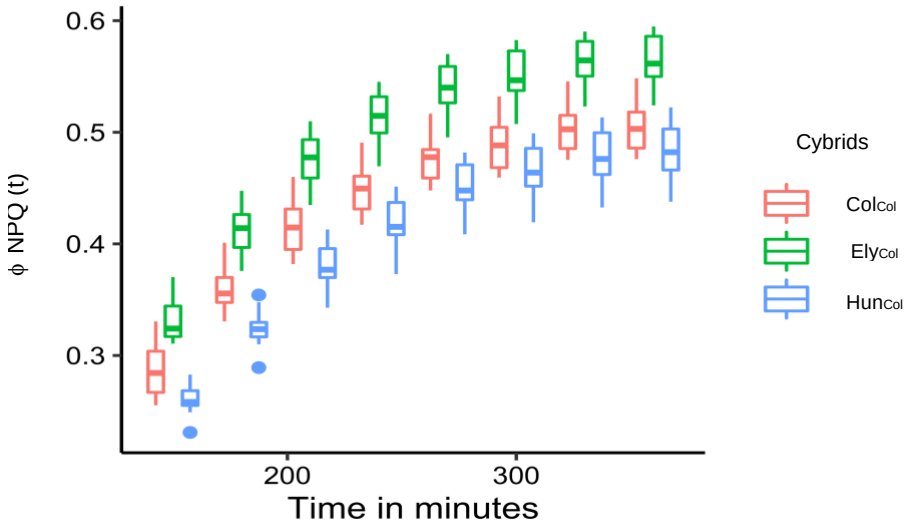

Figure 12: The variations of ϕNPQ(t) for the subset of high actinic light intensities used for NPQ(t), 605, 707, 793, 866, 924, 96, 991, 1000 µmol. m-2.s-1. ϕNPQ(t) is increasing when light intensity increases. The boxes of this figure can be read as the boxes of figure 7. The first group of boxes on the left represent the values of ϕNPQ(t) per cybrids when the actinic light intensity was 605 µmol. m-2. s-1, and this until 1000 µmol. m-2. s-1.

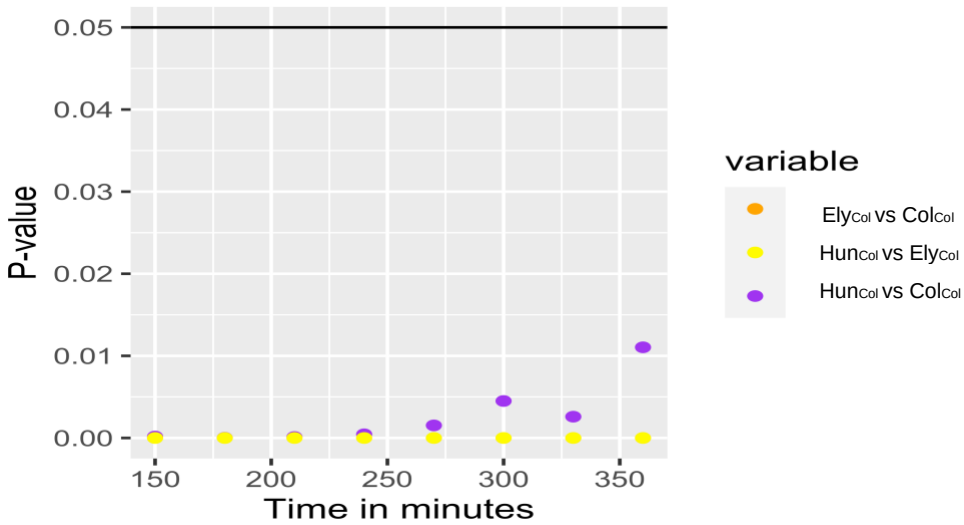

Figure 13: This figure represents the result of the posthoc test for the variations of ϕNPQ(t) between the cybrids for the subset of high light intensities. The black line represents the risk α fixed here at 0.05. The dots represent the results of the posthoc test. Each column of dots

represents one posthoc test for the three cybrids, per time point and so per light intensity. The first column on the left corresponds to the results of the posthoc test when the light intensity is 605 µmol. m-2. s-1, and then this pattern continues until 1000 µmol. m-2. s-1.

3.1.4 qE and qI

In the previous results, we have demonstrated that NPQ (estimated from NPQ(t)) was higher in Ely_{Col} compared to Hun_{Col} and Col_{Col}. As NPQ is divided into qE, and qI, we studied the presence or absence of correlation between a higher NPQ and a higher qE and/or qI. The variations of qE and qI were studied for the twenty-four light intensities. The outcomes of these measurements showed that when fluctuating the light intensity qE was higher in Ely_{Col} compared to Col_{Col} and Hun_{Col}, and this difference was exacerbated when the light intensity was higher than 500 µmol. m-2. s-1 (Figure 14). The results of the posthoc test were that after one-hundred thirty-five minutes qE was always significantly higher in Ely_{Col} compared to Col_{Col}, and always significantly higher in Ely_{Col} compared to Hun_{Col} after one-hundred sixty-five minutes (Figure 15). Concerning qE, in Hun_{Col} it was lower than qE of Col_{Col}, and the difference of qE between Hun_{Col} and Col_{Col} was almost always significant (Figure 15). Therefore, as for NPQ(t), the variations of qE were significantly higher in Ely_{Col} compared to Col_{Col} and Hun_{Col}, we plotted qE against NPQ(t) for this cybrid to establish whether they correlated (Figure 16). We notice that the relation is linear with an R-squared of 0.971 (Appendix 6, R-square qE/NPQ(t)). Therefore, we demonstrated from these results a positive and linear correlation between the higher NPQ(t) and the higher qE for Ely_{Col}.

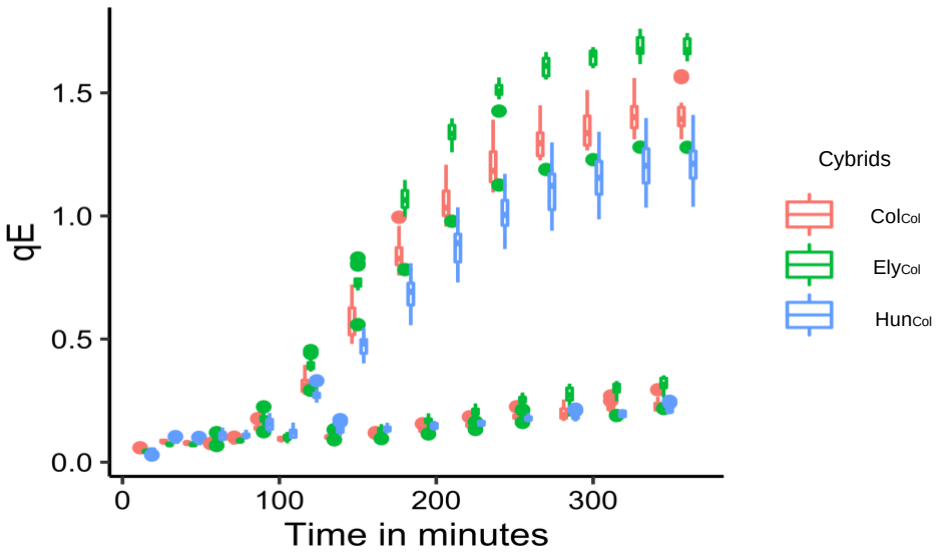

Figure 14: qE increases when the actinic light intensity increases. The boxes of this figure can be read as the boxes of figure 7. The first group of boxes on the left represent the values of qE when the actinic light intensity was 65 µmol. m-2. s-1 and this pattern continues until 1000 µmol. m-2. s-1.

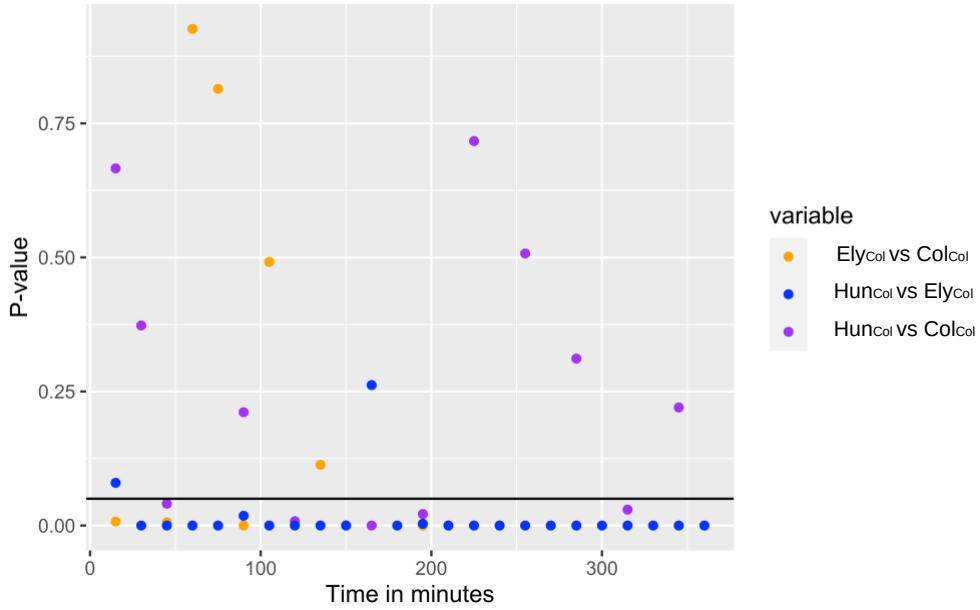

Figure 15:This figure represents the result of the posthoc test for the variations of qE between the cybrids for the twenty-four light intensities. The black line represents the risk α fixed here at 0.05. The dots represent the adjusted Tukey p-value obtained from the posthoc test. Each column of dots represents the results of the posthoc test for the three cybrids, per time point and so per light intensity. The first column on the left corresponds to the results of the posthoc test when the light intensity is 65 μmol. m^{-2}. s^{-1}, and then this pattern continues until 1000 μmol. m^{-2}. s^{-1}.

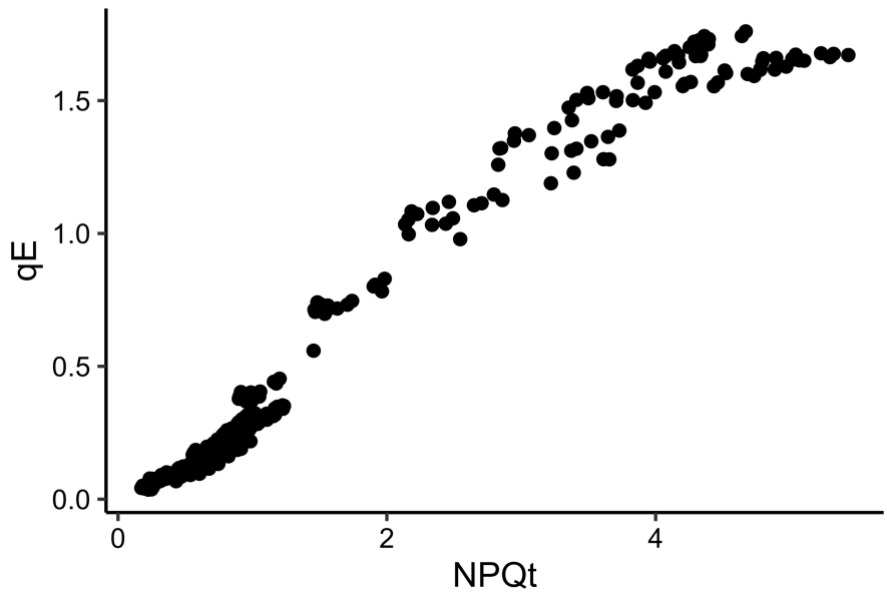

Figure 16:The variations of qE are represented in the function of the variations of NPQ(t), for the cybrid Ely_{Col}. Each dot represents the qE versus NPQ(t) value per individual per time point (seven individuals were used per batch and the results of the two batches were combined). The relationship between qE and NPQ(t) for Ely_{Col} is linear.

After studying the variations of qE for the twenty-four light intensities per cybrid, we studied the variations of qI. The value of qI was increasing through time. This increase was homogenous between cybrids, as, per time point, there was almost no variation of qI between the cybrids (Figure 17). The results of the posthoc test were that the difference of qI value between cybrids per time point was rarely significant (Figure 18). Moreover, by plotting qI against NPQ(t) (Figure 19) we obtain an R-square of 0.2255 (Appendix 6 R-square qI/NPQ(t)) which means that in this experiment there is no correlation between NPQ(t) and qI. It was also possible to notice that over a certain NPQ(t), qI was not anymore evolving for the three cybrids (Figure 19).

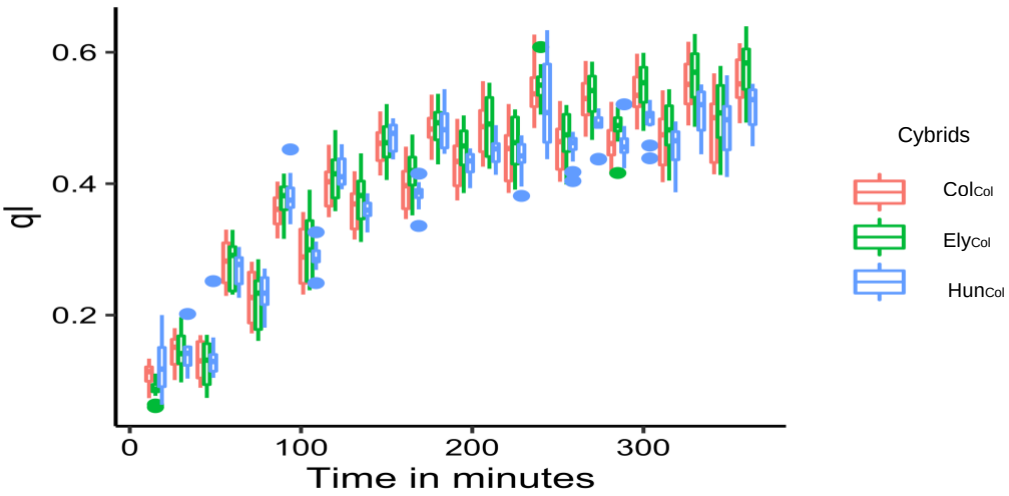

Figure 17: qI increases with the increase of the actinic light intensity. However, the increase of qI is more homogenous than the increase of qE. The boxes of this figure can be read as the boxes of figure 7. The first group boxes on the left represent the values of qI when the actinic light intensity was 65 µmol. m-2. s-1, and this until 1000 µmol. m-2. s-1.

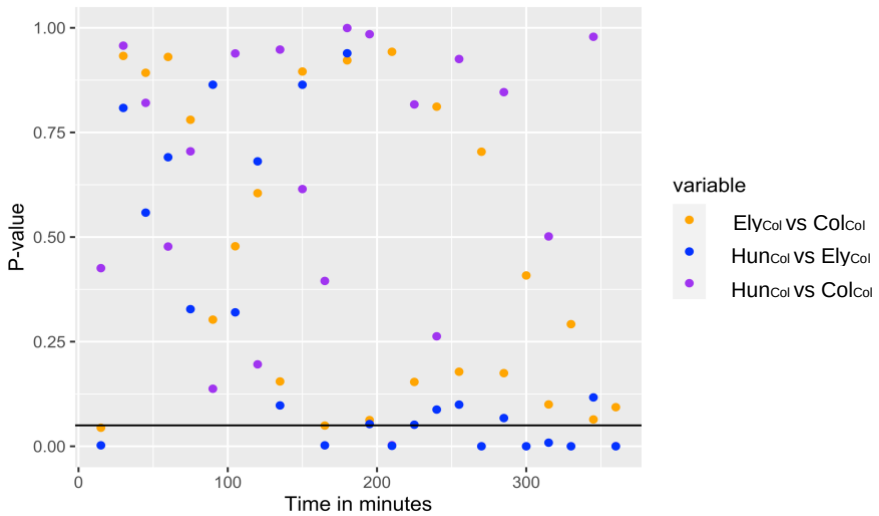

Figure18: This figure represents the result of the posthoc test for the variations of qI between the cybrids for the twenty-four light intensities. The black line represents the risk α fixed here at 0.05. The dots represent the adjusted Tukey p-value obtained from the posthoc test. Each

column of dots represents the results of the posthoc test for the three cybrids per time point and so per light intensity. The first column on the left corresponds to the results of the posthoc test when the light intensity is 65 µmol. m-2. s-1 and then this pattern continues until 1000 µmol. m-2. s-1.

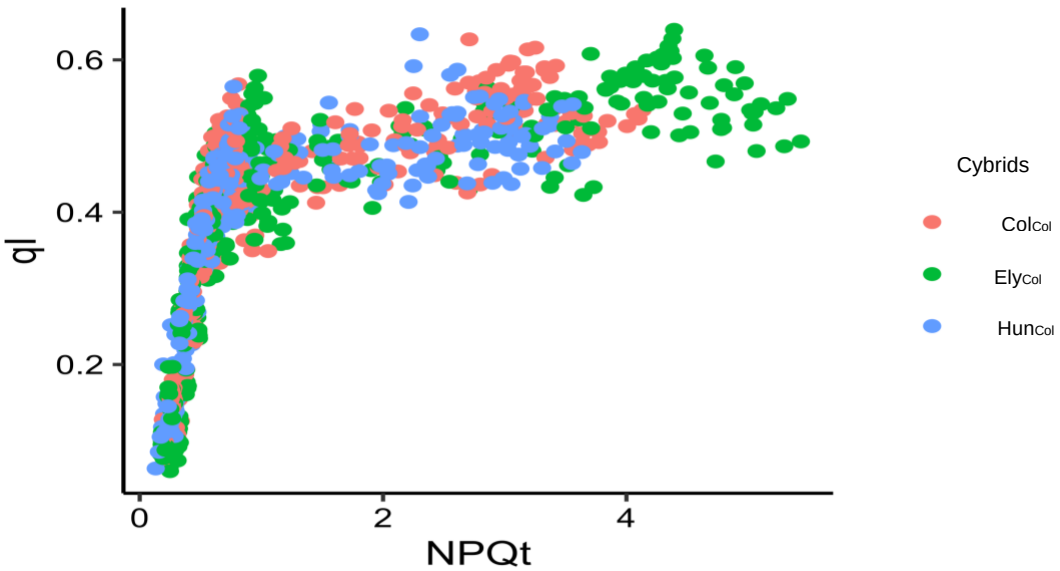

Figure 19: The variations of qI are represented in function of the variations of NPQ(t), for the three cybrids. Each dot represents the qI versus NPQ(t) value per individual (seven individuals were used per batch and the results of the two batches are combined) per time point. The relationship between qI and NPQ(t) for the three cybrids is not linear, from a certain point (NPQ(t) = 1) qI does not increase anymore.

3.2 NPQ relaxation

We have previously shown that in Ely_{Col} the higher NPQ(t) was correlated with a higher qE, which is the fast-relaxing component of NPQ. Then, to see how quickly the energy dissipated by NPQ was decreasing in Ely_{Col} and turned back into ϕPSII, we analysed the NPQ relaxation of Ely_{Col} and Col_{Col}. This experiment consisted of expressing the NPQ phenotype by fluctuating the actinic light intensities and then measure its relaxation at a low actinic light intensity and darkness. We kept a low light intensity because the VDE is light-dependent and complete darkness conditions are very rarely reached during a day. The results of the low actinic light intensity conditions are presented here, and the results of the dark conditions are presented in the appendix (Figures 33 to 35 Appendix 5). As Hun_{Col} presented neither a higher NPQ(t) nor a higher qE, we did not measure its relaxation.

3.2.1 The relaxation of NPQ

As the whole experiment only lasted 16 minutes between the F_m and the light relaxation, F_m and F_{mp} can be used directly to calculate NPQ, an estimation by NPQ(t) is not necessary. The first result of this experiment was that at the beginning of the relaxation period Ely_{Col} was presenting more NPQ than Col_{Col} (Figure 20A). However, by comparing the relaxation curve of NPQ for Ely_{Col} with the relaxation curve of NPQ for Col_{Col}, we could see that the curve of Ely_{Col} was decreasing faster (Figure 20A). This showed that the NPQ relaxation of Ely_{Col} was faster than the NPQ relaxation of NPQ of Col_{Col} and this for the hundred first seconds. By looking at the results of the ANOVA (Figure 20B), we could see that the difference between the NPQ relaxation of Ely_{Col} and Col_{Col} was almost always significant for the first hundred seconds. NPQ for Ely_{Col} was decreasing significantly faster than NPQ for Col_{Col} and this for the hundred first seconds.

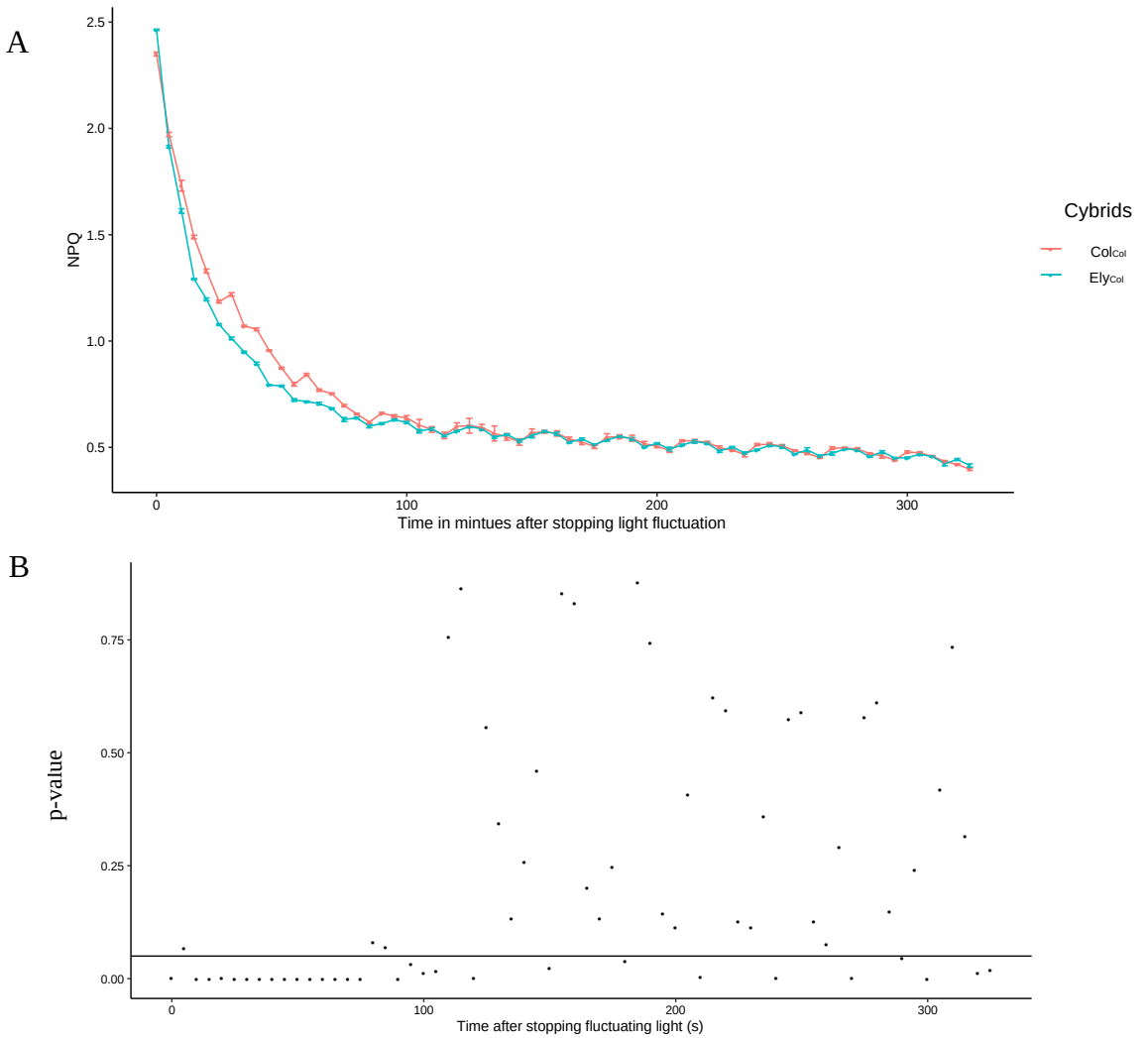

Figure 20: (A) The relaxation of NPQ through the time (after fifteen minutes of fluctuation of 1000 and 100 µmol. m^{-2}. s^{-1} (Figure 21 Appendix 3)) is represented here, the results of all the batches are combined. Each dot is the value of NPQ averaged over of the individual's NPQ values of the ten plants for each cybrid. (B) The results of the one-way ANOVA conducted per time point for the difference of NPQ between Col_{Col} and Ely_{Col} are represented here. The black line represents the risk α fixed here at 0.05. The difference of NPQ between the two cybrids is almost always significantly different for the first hundred seconds.

3.2.2 The increase of ϕPSII

The increase of ϕPSII was also monitored during the period of low light intensity (50 μmol m^{-2} s^{-1}), after the period of fluctuating light. From the results of this experiment, we could see that the value of ϕPSII for Ely_{Col} was lower at the beginning than the value of ϕPSII for Col_{Col}. This value was then higher from the third measurement (corresponding to ten seconds) until a hundred seconds (Figure 21A). Hence, the curve representing the value of ϕPSII for Ely_{Col} was increasing faster, thus, the level of ϕPSII increased faster in Ely_{Col} for the first hundred seconds. The results of the ANOVA were that the difference of ϕPSII between the two cybrids was very often significant during the first hundred seconds (Figure 21B). Therefore, during the hundred first seconds, the level of ϕPSII in Ely_{Col} was almost always significantly higher than the level of ϕPSII of Col_{Col}. These results mean that during the first hundred seconds, ϕPSII for Ely_{Col} was globally increasing significantly faster.

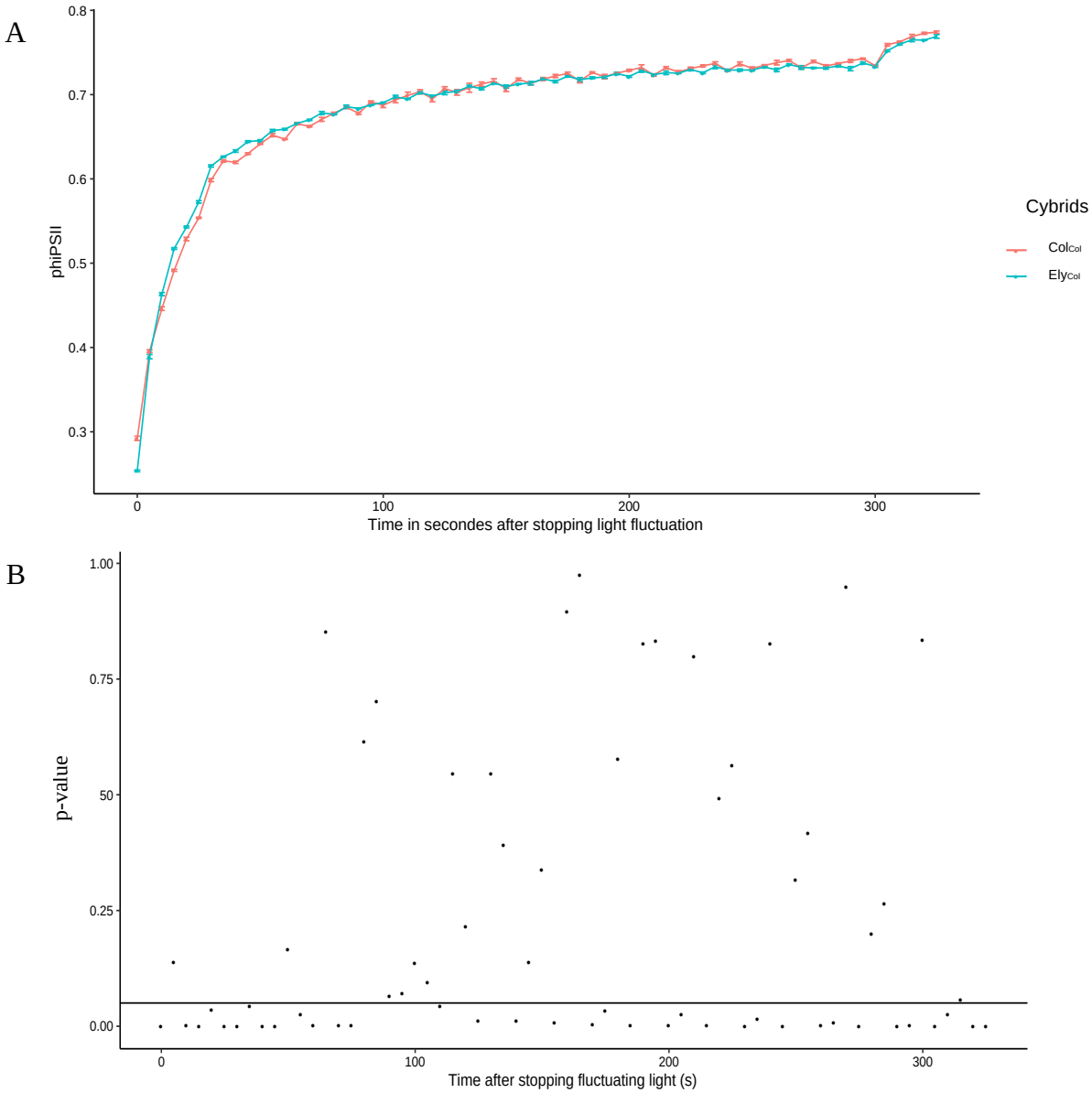

Figure 21: (A) The increase of ϕPSII through the time (after fifteen minutes of fluctuation of 1000 and 100 µmol. m-2. s- (cf. Appendix 3, figure 21)) is represented here, the results of all the batches are combined. Each dot is the value of ϕPSII averaged over of the individual's ϕPSII of the ten plants of each cybrid. (B) The results of the one-way ANOVA conducted per time point for the difference of ϕPSII between Col$_{Col}$ *and Ely*$_{Col}$ *are represented here. The black line represents the risk α fixed here at 0.05. The difference of ϕPSII between the two cybrids is almost always significantly different for the first hundred seconds.*

4 Discussion

4.1.1 The plasticity of the NPQ phenotype of Ely nucleotype can provide advantages for the plant under fluctuating light.

NPQ is a photoprotection mechanism, happening to eliminate as heat the excess of energy caused by an increase of light intensity. The apparition of NPQ is driven, in higher plants, by two sub-mechanisms (qE and qI) which induces conformational changes in the thylakoids membrane and pH changes in the thylakoid lumen (Müller et al. 2001). However, these conformational changes induced in the membrane are slower to disappear than they are to appear (Kromdijk et al. 2016). Thus, when the light intensity decreases there is a decay in NPQ disappearance leading to a reduction of ϕPSII and further of the yield (Kromdijk et al. 2016). Then, higher yield could be obtained by fastening the relaxation of NPQ which further fastens the increase in ϕPSII (Kromdijk et al. 2016; Long et al. 2006; Murchie and Niyogi 2011).

The study of NPQ plasticity under fluctuating light conditions has demonstrated that the nucleus of the Ely accession was producing a higher rate of NPQ compared to almost all the cybrids of the panel (Flood et al. 2020). The results of our fluctuating light response curve correlated with this previous founding since NPQ(t) of Ely_{Col} was significantly higher than NPQ(t) of Col_{Col} and Hun_{Col} (Figures 7 and 8). In our study, the calculation of NPQ was, however, replaced by the calculation of NPQ(t). The use of NPQ(t) permitted to arise any phenotypic variations due to qI accumulation, chloroplast and leaves movement occurring during the seven hours of the experiment (Tietz et al. 2017). Then the phenotypic variations observed here were solely due to NPQ variations. Moreover, by measuring the variations of qE, the fastest relaxing and dominant sub-mechanism of NPQ (Dall'Osto et al. 2014), for the twenty-four light intensities of the fluctuating light response curve we noticed that qE was significantly higher in Ely_{Col} (Figures 14 and 15). The correlation plot established from the result of the experiment showed that in Ely_{Col} the higher rate of NPQ(t) correlated with a higher rate of qE (Figure 19). Therefore, it seems that the origin of a higher NPQ(t) visible in Ely_{Col} comes from a higher qE.

The Ely nucleus by generating more qE might provide two major advantages to the plant. The results of a previous study have already linked a higher level of qE to a faster synthetizing and relaxing NPQ (Kromdijk et al. 2016). This experiment has been conducted in tobacco *VPZ* mutant lines which were showing overexpression of the genes coding for the PsbS protein, VDE, and ZEP. By overexpressing these genes, the VPZ lines were presenting a higher qE and then a faster relaxing NPQ under dark conditions and after exposure to fluctuating light. These results are following the results found in our second experiment, the NPQ relaxation. In this experiment, the kinetics of NPQ relaxation was monitored at low light intensity (50 µmol. m^{-2}. s^{-1}) and darkness after having been expressed by exposing the cybrids to fluctuating light intensity. The outcomes of the NPQ relaxation were that the NPQ relaxation for Ely_{Col}, which possesses more qE than Col_{Col}, was faster than the NPQ relaxation for Col_{Col}. This result was found during the first hundred seconds of relaxation phase at low light intensity (Figure 20 A

and B) and during the first one-hundred-fifty seconds in the dark (Figures 33 and 35 Appendix 5). The lower the light intensity will be the more NPQ will disappear, that is why in the dark the relaxation of NPQ is more important (Kress and Jahns 2017). Thus, the first advantage provided by a higher qE would be to make the disappearance of NPQ faster under decreasing light intensity conditions, after exposure to fluctuating light intensity. Furthermore, studies conducted on *npq1* and *npq4* mutants which were lacking of certain qE elements, showed that these mutants were having a delay in synthetizing NPQ which make them lighter sensitive (Dall'Osto et al. 2014; Ikeuchi, Sato, and Endo 2016; Niyogi et al. 1998). Then, a second advantage provided to the plant by a higher level of qE would synthetize NPQ faster under high light intensity conditions, hence, better protection under fluctuating light intensity.

Additionally, our NPQ relaxation experiment's results showed a correlation between the faster decrease of NPQ in Ely_{Col} and a faster increase of ϕPSII in this same cybrid, during the first hundred seconds of the relaxation phase (Figure 21 A and B). Nonetheless, even though, the value of ϕPSII resulted from the average ten individuals for each cybrid, only one measurement before each saturating pulse was done to measure F_P. By repeating the experiments and adding more measurements for ϕPSII a firm conclusion of the results can be drawn. While, our low number of values for the measurement of F_P, our results were still coherent with those found for the *VPZ* lines in tobacco (Kromdijk et al. 2016). The *VPZ* mutant lines by having a faster relaxing NPQ were presenting a faster increase of ϕPSII compared to the WT (Kromdijk et al. 2016). In this study, the scientists went even further in demonstrating the benefits of a faster relaxing NPQ under fluctuating light, by monitoring the maximum efficiency of CO2 assimilation (ϕCO_2) and further on the biomass productivity. They showed that the biomass productivity of the *VPZ* lines has augmented of 15% compared to the control (WT) (Kromdijk et al. 2016). Nonetheless, this study also reported that under steady high light conditions possessing this trait will probably not be beneficial for the plant as more energy will be lost as heat. As in our results, we found that the NPQ(t) of Ely nucleus was also higher compared to the NPQ(t) of the other cybrids (Figures 7 and 9), we can also conclude that possessing this trait would not be beneficial under steady light intensity conditions. Therefore, from these results, it seems that the NPQ phenotype of the Ely nucleus would be a beneficial trait to possess for the plant but uniquely under fluctuating light conditions.

However, another study drew different conclusions by using the same VPZ construct but in *A. thaliana* (Garcia-Molina and Leister 2020). In this experiment despite a faster relaxation of NPQ in the *VPZ* mutant lines compared to wild type lines, an increase of biomass was not visible (Garcia-Molina and Leister 2020). The authors even reported a decrease in the total biomass in *VZP* lines compared to the control, in certain light growing conditions. To explain the decline of *A. thaliana VPZ* lines biomass, despite a faster relaxation of NPQ, two mechanisms were put toward by the authors of the article. First, it could be that a modification in the level of energy released by NPQ, could affect other mechanisms controlling the repartition of the energy over the thylakoid membrane. Another, explanation to the reduction of biomass in the *A. thaliana VPZ* lines, can be that the artificial increase of ϕCO_2 was not followed by an increase in nitrogen uptake, while nitrogen is a limiting element for growth.

Moreover, the organs of the plants where the carbons are normally allocated can be saturated by an increase of carbons input. These two phenomena combined lead to a down-regulation of photosynthesis (Sinclair, Rufty, and Lewis 2019). Thus, it could be that if other bottlenecks are present somewhere else in the biomass formation process, the faster relaxing NPQ of Ely nucleus, leading to a faster increasing ϕPSII, would not be sufficient to increase the yield.

That is why, regarding the experiments carried out in our study and the results of these two previous studies, several steps still need to be undertaken to entirely conclude on the benefit of the faster relaxing NPQ phenotype of Ely nucleus. First, in our study, the entire Ely nucleus has been introduced in Col plasmotype, hence, the NPQ phenotypic variations that we have observed are not uniquely due to the varying elements of Ely nucleus. Thus, to assess solely the effect of this varying element of Ely nucleus causing the specific NPQ phenotype, this varying element should first be isolated and then inserted into Col WT. The varying element of Ely nucleus can be found through the QTL map currently realised in the Laboratory of Genetics from a Col *CENH3* mutant and an Ely WT. Then, the NPQ phenotype of the transgenic Col should be compared with those of non-modified Col WT (used as a control). This step would serve to only assess the effects of the varying element of Ely nucleus on the variations of the NPQ phenotype. Moreover, in both of the studies presented above (Garcia-Molina and Leister 2020; Kromdijk et al. 2016), the plants have been grown under fluctuating light intensity, because this parameter is necessary for the expression of the NPQ phenotype (Cruz et al. 2016). However, in our study the *A. thaliana* plants have been grown under steady light, the NPQ phenotype was only expressed in the experiment by fluctuating the light intensity. Therefore, to fully assess the effects of the varying element of Ely nucleus on the NPQ phenotype, the future transgenics Col, should also be grown in a fluctuating light environment. Ideally, the fluctuating light should be natural so the experiment should be performed in a field, however, in those conditions it is harder to control the other parameters of growth. Thus, a first experiment can be realised in a greenhouse and the results can be confirmed or invalidated by a field experiment. This would enable the monitoring of the complete effect of the NPQ phenotype due to the varying element of Ely nucleus. Last but not least ϕPSII, ϕCO_2, and the biomass should be monitored on Col, containing Ely nucleus variation, grown in a fluctuating light environment, and compared with those of Col WT. As bottlenecks can happen between the photosynthesis and the final yield formation, the values of these parameters compared to those of the WT will give the final answer regarding the benefice of Ely nucleus NPQ.

Unlike the correlation between the increase of NPQ(t) and qE saw for Ely_{Col}, a correlation between the increase of NPQ(t) and an increase of qI for this cybrid could not be established from our results. Thus, an increase of NPQ in Ely_{Col} will not be associated with a higher qI compared to Col_{Col} and Hun_{Col}. No comparison of this result could have been found in the literature.

4.1.2 NPQ seems to have its own regulation mechanism

Previous researches have categorized NPQ as a mechanism caused uniquely by a down-regulation of ϕPSII (Kramer et al. 2004) and photosynthesis and NPQ as very conserved mechanisms among the plant species (Arntz and Delph 2001; Demmig-adams et al. 2014). In our study, the cybrids used (Ely_{Col}, Col_{Col}, and Hun_{Col}) were all containing the same plasmotype (Col) which does not possess *psbA* mutation. The mutated *psbA* gene, leading to a decrease of ϕPSII, is contained in Ely and Hun chloroplast genome (El-Lithy et al. 2005; Harbinson and Aarts 2015). The particularity of Ely nucleus is to compensate for the low ϕPSII by high NPQ coming from a nuclear regulation (Flood et al. 2020). Therefore, by adding Ely nucleus into Col plasmotype, the nucleus does need to compensate for the low ϕPSII by increasing NPQ. Additionally, as all cybrids were containing the same Col plasmotype, for certain a light intensity, the three cybrids were expected to present the same level of ϕPSII. Then, following the statement that NPQ is caused by a decrease of ϕPSII, for a given light intensity, the three cybrids should produce the same level of NPQ. Furthermore, as ϕPSII and NPQ are supposed to be conserved mechanisms, the variations of the ratio ϕPSII/NPQ through the fluctuation of the light intensity should stay constant between the three cybrids. However, by studying the variations of ϕPSII/NPQ(t) for the subset of high light intensities, we found that for the same level of ϕPSII, Ely_{Col} was producing more NPQ(t) than Col_{Col} and Hun_{Col} (Figure 9B). We did this experiment on a subset of high light intensities because NPQ is then more expressed (Horton and Hague 1988). Moreover, the variations of the ratio ϕPSII/NPQ(t) for the subset of high light intensities for each cybrid, represented by the values of the slopes, were significantly different from the others (Table 1). These results mean first that the NPQ mechanism is differently regulated by each cybrid and then that through the decrease or increase of light intensity, the difference between the cybrids for the ratio ϕPSII/NPQ(t) does not stay constant. These results do not align with the previous founding. If NPQ was caused only by a decrease of ϕPSII, then the level of NPQ should have been the same among the cybrids. If ϕPSII and NPQ were perfectly conserved among species and within species, then the difference for the ϕPSII/NPQ(t) should have been constant between the three cybrids through the variations of light intensity. Therefore, we could not affirm from our results that NPQ was caused uniquely by a down-regulation of ϕPSII. On the contrary, we found that NPQ seems to have its own mechanism of regulation.

Since NPQ does not vary in the same way among the cybrids as it was expected to do, we investigated further the origin of NPQ variations. NPQ is the result of the ratio ϕNO/ ϕNPQ, hence, we studied independently the variations of these two parameters. ϕNO is the non-regulated heat-dissipation and fluorescence emission, ϕNPQ is the thermal-energy dissipated linked to NPQ and ϕNPQ+ϕNO+ϕPSII=1. As we estimated NPQ from NPQ(t), for the same reasons we estimated ϕNO from ϕNO(t) and ϕNPQ from ϕNPQ(t). To study the variations of ϕNO(t) and ϕNPQ(t) we used the same subset of high light intensities as for the ratio ϕPSII/NPQ(t). The outcomes of this analysis were that the higher rate of NPQ(t) in Ely_{Col} was due to a significantly lower ϕNO(t) (Figures 12 and 13) and a significantly higher ϕNPQ(t)

(Figure 14 and 15). These results are coherent with statements previously emitted on literature where it is said that under fluctuating light conditions, a higher ϕNPQ can be sufficient to compensate for the decrease of ϕPSII and then could lower ϕNO (Klughammer and Schreiber 2008).

Among the cybrids, used in this study, NPQ (calculated from NPQ(t)) is differently regulated and we could hypothesis that this result can be extended to plants species in general. However, the conformational changes induced to produce NPQ are well conserved among the plants' species (Demmig-adams et al. 2014). It is likely that the genes regulating NPQ are well conserved among species but are differentially expressed by the different plants' species. This hypothesis correlates with the results from the *npq1*, *npq2*, and *npq4* mutants. The *npq1* and *npq2* mutants, respectively knock-down mutants for the violaxanthin deepoxidase and the zeaxanthin epoxidase, were presenting a reduced NPQ (Niyogi et al. 1998). The *npq4* mutant by synthetizing way less PsbS protein than the WT *A. thaliana* was also having less NPQ (Khuong, Robaglia, and Caffarri 2019). A similar correlation can be established with the *VPZ* tobacco mutants, which by overexpressing genes regulating for VDE, ZEP, and PsbS were producing faster synthetizing and relaxing NPQ (Kromdijk et al. 2016). Thus, as Ely nucleus gives a higher NPQ it is highly probable that one or several genes regulating the conformational changes of NPQ is(are) differently regulated in this nucleus. Thus, the higher NPQ we see would be due to a difference in the amount of conformational change induced or even in modifications of conformational changes.

Nonetheless, our results only permitted to demonstrated that NPQ has up-regulated in Ely thanks to a chlorophyll fluorescence phenotyping experiment. Then, to verify the above hypothesis, the results of the QTL map established from the doubled-haploid population made from Col CENH3 mutant and Ely WT have to be used. An alternative option would be to sequence the Ely nucleus and compared this sequence with the nucleus sequence of Col, starting by the genes already known to regulate NPQ formation. In both cases, the level of conformational changes (especially PsbS protein synthesis and xanthophyll cycle) happening in the thylakoid membrane when Ely nucleus is expressed should be analysed. The phenotypic and genotypic data should be gathered to reveal the genes of Ely nucleus underlying the regulation of conformational change giving a higher NPQ.

4.2 A different NPQ phenotype for Hun^{Col}

In this study, we have first demonstrated that, under fluctuating light conditions, NPQ was upregulated by the nucleus of Ely. Then, that this higher NPQ is correlated with the upregulation of qE. This upregulation of qE leads, when light intensity decreases, to a faster relaxing NPQ and further to a faster increasing ϕPSII. However, from this study of the NPQ phenotype of Ely nucleus, we could not obtain information on whether the Ely nucleus variation is crucial for the survival of Ely WT. In other words, if the Ely nucleus variation happens to compensate a *psbA* mutation (a beneficial mutation), or if this variation was present before the *psbA* mutation. Previously it has been found that the *psbA* mutation always coincided with the

same nucleotype (Flood et al. 2016). This could be explained by a strong dependency on a beneficial mutation happening in the nucleus and the *psbA* mutation or because of a lack of outcrossing (Flood et al. 2016). Lately, the accession Hunley possessing a *psbA* mutation but a different nucleus has been discovered. Before our work, the NPQ phenotype of the Hun nucleus has not been studied.

Therefore, in this study, we have introduced Hun and Ely nucleus into the Col plasmotype to study the effect of the Hun and Ely nucleus on the NPQ phenotype independently of ϕPSII variations. During the fluctuating light response curve experiment, the NPQ phenotypic variations of the Hun nucleus were compared with those of Ely nucleus. By comparing the results of the NPQ phenotypes, we were expecting to get insight into the origin of the variation of Ely nucleus. If Hun nucleus would have given the same NPQ phenotype as Ely nucleus we could have hypothesised that the nucleus of Hun and Ely would have contained the same nucleic variation. This statement would have led to the hypothesis that the variation of Ely nucleus was an adaptation to a *psbA* mutation, and was a beneficial mutation that got fixed. On the contrary, if the Hun nucleus would not possess the same nucleic variation as Ely, it would let us assume that the variation of the Ely nucleus is a neutral evolution, which could have happened before a *psbA* mutation.

The results of the NPQ phenotype of the Hun nucleus did not correlate with the results of the NPQ phenotype of Ely nucleus (Figures 7, 8, and 9A and B). Unlike Ely nucleus, the Hun nucleus was presenting a lower NPQ than Col_{Col}. As Hun nucleus did not present the same NPQ phenotype as Ely nucleus NPQ phenotype, we hypothesized that the Hun nucleus did not possess the same nucleic variation as Ely. Nonetheless, this conclusion cannot fully be made without sequencing the nucleus of Hun and comparing this genetic sequence with the genetic sequence of Ely nucleus. Even though the conclusion could not be fully established from our results, the outcomes of this experiment still oriented our hypothesis on the fact that Ely nucleus variation could have happened before the *psbA* mutation or even be a neutral evolution.

However, the hypothesis of a neutral evolution seems not to be coherent with the results we obtained, as, under fluctuating light, the NPQ phenotype of Ely nucleus appears to increase the fitness of Ely_{Col}. Ely nucleus is providing the plant with faster and more flexible NPQ leading to faster photoprotection when the light intensity is increasing, and a faster increase in ϕPSII when the light intensity is decreasing. Thus, by looking only at the phenotyping results of NPQ and ϕPSII, it seems that the Ely nucleus increases the capacity of the plant to survive. Nonetheless, this statement stays hypothetical until further experiments will be done to analysis the effects on the plants of the Ely nucleus NPQ phenotype. But, this would mean that the variation in Ely nucleus by producing more NPQ would, instead, be a beneficial mutation and get fixed by hitchhiking with a *psbA* mutation. This hypothesis seems also more logical considering previous results showing that the *psbA* mutate gene always inherited with the same nucleus, which is the result of a fast selection on a beneficial mutation (Flood et al. 2016). Concerning the other hypothesis stating that the Ely nucleus variation leading to a higher NPQ

was present before the *psbA* mutation, uncertainties remain. Why would a plant keep a trait which makes it lose more energy as heat while it has efficient ϕPSII ?

Therefore, regarding all these results and the divergence of hypotheses that they generate, two scenarios arose. First, it can be that the *psbA* mutation happens later in Hun chloroplast genome compared to Ely chloroplast genome and that the nucleus of Hun did not have the time to adapt to this mutation yet. The other scenario would be that the variation of Ely nucleus was present before the *psbA* mutation, which could explain the absence of a similar NPQ phenotype from the Hun nucleus. Therefore, regarding all these hypotheses and at the results of our experiments too much uncertainty remains to let us orientate our hypothesis on whether the origin of the variation of Ely nucleus is an adaptation to the *psbA* mutation or was present before it.

5 Conclusion

My thesis aimed to answer two questions, first, whether the variation of Ely nucleus was an adaptation to the *psbA* mutation or a neutral evolution, second, whether he NPQ phenotype of Ely nucleus is a beneficial trait to have for the plant. To answer these questions, two phenotyping experiments were carried out. The results obtained permitted to draw several conclusions.

From the results of the fluctuating light response curve, it was established that the NPQ was independently regulated by the different cybrids and that this mechanism was active and not passive. To fully conclude on this statement the genetics underlying NPQ should be revealed and the different levels of expression of the genes between the accessions should be monitored.

The second result of the fluctuating light response curve is the correlation between the high NPQ and an elevation of qE for the cybrid Ely_{Col}, this result aligned with statements made in previous experiments. With the NPQ relaxation curve, the physiology of the NPQ phenotype of Ely_{Col} and especially the relaxation kinetics was investigated. From the results of this experiment, the conclusion was that a higher qE was correlated with a faster relaxation of NPQ leading to a faster increase of ϕPSII when the light intensity was decreasing. Furthermore, according to previous studies, possessing more qE could help to faster synthetized NPQ and then provide a better photoprotection. Regarding these results, it seems that the NPQ phenotype of the Ely nucleus will be a beneficial trait to have for the plant under fluctuating light conditions. However, to fully conclude on this statement further experiments need to be carried out, to test whether further bottlenecks in the photosynthetic pathway and the allocation of energy will not impede the increase of biomass productivity, which is the final breeding goal.

The question of the origin of the nucleic variation in Ely was addressed by comparing the NPQ phenotype of Ely nucleus results with those of the Hun nucleus. Hun is possessing a *psbA* mutation in the chloroplast genome but a different nucleus of Ely. By comparing the NPQ phenotypes originating from these two nuclei, the conclusion was that the NPQ phenotypes were slightly different for the two cybrids. Hence, it is likely that Hun does not possess the same nucleic variation as Ely. This result does not support the hypothesis of an adaptation of the Ely nucleus to the *psbA* mutation. However, from the phenotypic results of the two experiments, it seems that the variation of Ely nucleus by increasing the plasticity of the NPQ phenotype, provides a higher fitness to Ely accession, compared to an accession with the *psbA* mutation and without NPQ compensation. These results are corroborated by the fact that the *psbA* mutation was always found with the same nuclear background leading to a higher NPQ, the sign of a selection for a beneficial trait. Thus, it could be that this nucleic variation, which seems beneficial, happens to compensate for the low ϕPSII or was present before the *psbA* mutation. But having the NPQ phenotype of Ely nucleus without the *psbA* mutation in the chloroplast genome does not seem to beneficial for the plant as more energy will be lost as heat

while ϕPSII is efficient. Therefore, from our results, it is still not possible to orient our hypothesis on the origin of the Ely nucleus compared to the *psbA* mutation.

Acknowledgments

I would like to thanks particularly Tom Theeuwen, for his constant help and his patience all along with my thesis. It has been a real opportunity to work on this project, I learned a lot even on disciplines I was not expecting to. It was a very enriching and constructive experience.

I also thanks to Mark Aarts, for his constructive feedback and advice on my work, Bas Zwaan for accepting to be my final examiner, and Jeremy Harbison for his help on questions regarding the physiological aspect of my work.

My final thanks go to the team of the Laboratory of Genetics, it has been a pleasure to work with them.

Dankjewel !

References

Allen, John F. 2003. “State Transitions - A Question of Balance.” *Science*.

Alonso-Blanco, Carlos, and Maarten Koornneef. 2000. “Naturally Occurring Variation in Arabidopsis: An Underexploited Resource for Plant Genetics.” *Trends in Plant Science*.

Anon. 2009. *Climate Change : Impact on Agriculture and Costs of Adaptation*.

Anon. 2018. “Chlorophyll Fluorescence as a Tool for Describing the Operation and Regulation of Photosynthesis in Vivo.” in *Light Harvesting in Photosynthesis*.

Arber, Werner. 2010. “Genetic Engineering Compared to Natural Genetic Variations.” *New Biotechnology*.

Arntz, Michele A. and Lynda F. Delph. 2001. “Pattern and Process: Evidence for the Evolution of Photosynthetic Traits in Natural Populations.” *Oecologia* 127(4):455–67.

Baker, Neil R. 2008. “Chlorophyll Fluorescence: A Probe of Photosynthesis In Vivo.” *Annual Review of Plant Biology*.

Ballottari, Matteo, Julien Girardon, Luca Dall’Osto, and Roberto Bassi. 2012. “Evolution and Functional Properties of Photosystem II Light Harvesting Complexes in Eukaryotes.” *Biochimica et Biophysica Acta - Bioenergetics*.

Bellan, Alessandra, Francesca Bucci, Giorgio Perin, Alessandro Alboresi, and Tomas Morosinotto. 2020. “Photosynthesis Regulation in Response to Fluctuating Light in the Secondary Endosymbiont Alga Nannochloropsis Gaditana.” *Plant and Cell Physiology* 61(1):41–52.

Bradbury, Michael and Neil R. Baker. 1984. “A Quantitative Determination of Photochemical and Non-Photochemical Quenching during the Slow Phase of the Chlorophyll Fluorescence Induction Curve of Bean Leaves.” *BBA - Bioenergetics*.

Britt, Anne B. and Sundaram Kuppu. 2016. “Cenh3: An Emerging Player in Haploid Induction Technology.” *Frontiers in Plant Science*.

Budar, Françoise and Sota Fujii. 2012. “Cytonuclear Adaptation in Plants.” in *Advances in Botanical Research*.

Cleland, Robyn E., Anastasios Melis, and Patrick J. Neale. 1986. “Mechanism of Photoinhibition: Photochemical Reaction Center Inactivation in System II of Chloroplasts.” *Photosynthesis Research*.

Cruz, Jeffrey A., Linda J. Savage, Robert Zegarac, Christopher C. Hall, Mio Satoh-Cruz, Geoffry A. Davis, William Kent Kovac, Jin Chen, and David M. Kramer. 2016a. “Dynamic Environmental Photosynthetic Imaging Reveals Emergent Phenotypes.” *Cell Systems*.

Cruz, Jeffrey A., Linda J. Savage, Robert Zegarac, Christopher C. Hall, Mio Satoh-Cruz, Geoffry A. Davis, William Kent Kovac, Jin Chen, and David M. Kramer. 2016b. “Dynamic Environmental Photosynthetic Imaging Reveals Emergent Phenotypes.” *Cell Systems*.

Dall’Osto, Luca, Stefano Cazzaniga, Masamitsu Wada, and Roberto Bassi. 2014. “On the Origin of a Slowly Reversible Fluorescence Decay Component in the Arabidopsis Npq4 Mutant.” *Philosophical Transactions of the Royal Society B: Biological Sciences*.

Demmig-Adams, Barbara. 1998. “Survey of Thermal Energy Dissipation and Pigment

Composition in Sun and Shade Leaves." *Plant and Cell Physiology*.

Demmig-Adams, Barbara, William W. Adams, Volker Ebbert, and Barry A. Logan. 1999. "Ecophysiology of the Xanthophyll Cycle."

Demmig-adams, Barbara, Christopher M. Cohu, Jared J. Stewart, and William W. Adams Iii. 2014. "Non-Photochemical Quenching and Energy Dissipation in Plants, Algae and Cyanobacteria." *Photosynthesis and Respiration*.

El-Lithy, Mohamed E., Gustavo C. Rodrigues, Jack J. S. Van Rensen, Jan F. H. Snel, Hans J. H. A. Dassen, Maarten Koornneef, Marcel A. K. Jansen, Mark G. M. Aarts, and Dick Vreugdenhil. 2005. "Altered Photosynthetic Performance of a Natural Arabidopsis Accession Is Associated with Atrazine Resistance." *Journal of Experimental Botany*.

Flood, Pádraic J., Joost Van Heerwaarden, Frank Becker, C. Bastiaan De Snoo, Jeremy Harbinson, and Mark G. M. Aarts. 2016. "Whole-Genome Hitchhiking on an Organelle Mutation." *Current Biology* 26(10):1306–11.

Flood, Pádraic J., Tom P. J. M. Theeuwen, Korbinian Schneeberger, Paul Keizer, Willem Kruijer, Edouard Severing, Evangelos Kouklas, Jos A. Hageman, Frank F. M. Becker, Sabine K. K. Schnabel, Leo Willems, Wilco Ligterink, Jeroen van Arkel, Roland Mumm, José M. Gualberto, Linda Savage, David M. Kramer, Joost J. B. Keurentjes, Fred van Eeuwijk, Maarten Koornneef, Jeremy Harbinson, Mark G. M. Aarts, and Erik Wijnker. 2020. "Reciprocal Cybrids Reveal How Organellar Genomes Affect Plant Phenotypes." *BioRxiv* (trez).

Foyer, Christine H. and Shigeru Shigeoka. 2011. "Understanding Oxidative Stress and Antioxidant Functions to Enhance Photosynthesis." *Plant Physiology*.

Gao, Jinlan, Hao Wang, Qipeng Yuan, and Yue Feng. 2018. "Structure and Function of the Photosystem Supercomplexes." *Frontiers in Plant Science*.

Garcia-Molina, Antoni and Dario Leister. 2020. "Accelerated Relaxation of Photoprotection Impairs Biomass Accumulation in Arabidopsis." *Nature Plants* 6(1):9–12.

Greiner, Stephan and Ralph Bock. 2013. "Tuning a Ménage à Trois: Co-Evolution and Co-Adaptation of Nuclear and Organellar Genomes in Plants." *BioEssays*.

Harbinson, Jeremy and Mark G. M. Aarts. 2015. *Natural Genetic Variation in Arabidopsis Thaliana Photosynthesis - Chapter 1, 2 & 4*. Vol. 16.

Horton, Peter and Alan Hague. 1988. "Studies on the Induction of Chlorophyll Fluorescence in Isolated Barley Protoplasts. IV. Resolution of Non-Photochemical Quenching." *BBA - Bioenergetics*.

Ikeuchi, Masahiro, Fumihiko Sato, and Tsuyoshi Endo. 2016. "Allocation of Absorbed Light Energy in Photosystem II in NPQ Mutants of Arabidopsis." *Plant and Cell Physiology*.

JOHNSON, G. N., A. J. YOUNG, J. D. SCHOLES, and P. HORTON. 1993. "The Dissipation of Excess Excitation Energy in British Plant Species." *Plant, Cell & Environment*.

Joseph, Bindu, Jason A. Corwin, Tobias Züst, Baohua Li, Majid Iravani, Gabriela Schaepman-Strub, Lindsay A. Turnbull, and Daniel J. Kliebensteina. 2013. "Hierarchical Nuclear and Cytoplasmic Genetic Architectures for Plant Growth and Defense within Arabidopsis." *Plant Cell*.

Jung, Hou Sung and Krishna K. Niyogi. 2009. "Quantitative Genetic Analysis of Thermal Dissipation in Arabidopsis 1[W][OA]." *Plant Physiology*.

Kasajima, Ichiro, Kaworu Ebana, Toshio Yamamoto, Kentaro Takahara, Masahiro Yano,

Maki Kawai-Yamada, and Hirofumi Uchimiya. 2011. “Molecular Distinction in Genetic Regulation of Nonphotochemical Quenching in Rice.” *Proceedings of the National Academy of Sciences of the United States of America*.

Khuong, Thi Thu Huong, Christophe Robaglia, and Stefano Caffarri. 2019. “Photoprotection and Growth under Different Lights of Arabidopsis Single and Double Mutants for Energy Dissipation (Npq4) and State Transitions (Pph1).” *Plant Cell Reports*.

Klughammer, Christof and Ulrich Schreiber. 2008. “Complementary PS II Quantum Yields Calculated from Simple Fluorescence Parameters Measured by PAM Fluorometry and the Saturation Pulse Method.” *PAM Application Notes* 1(1):27–35.

Kramer, David M., Giles Johnson, Olavi Kiirats, and Gerald E. Edwards. 2004. “New Fluorescence Parameters for the Determination of QA Redox State and Excitation Energy Fluxes.” *Photosynthesis Research*.

Krause, G. H. and E. Weis. 1991. “Chlorophyll Fluorescence and Photosynthesis: The Basics.” *Annual Review of Plant Physiology and Plant Molecular Biology*.

Kress, Eugen and Peter Jahns. 2017. “The Dynamics of Energy Dissipation and Xanthophyll Conversion in Arabidopsis Indicate an Indirect Photoprotective Role of Zeaxanthin in Slowly Inducible and Relaxing Components of Non-Photochemical Quenching of Excitation Energy.” *Frontiers in Plant Science*.

Kromdijk, Johannes, Katarzyna Głowacka, Lauriebeth Leonelli, Stéphane T. Gabilly, Masakazu Iwai, Krishna K. Niyogi, and Stephen P. Long. 2016. “Improving Photosynthesis and Crop Productivity by Accelerating Recovery from Photoprotection.” *Science*.

Kromdijk, Johannes and Stephen P. Long. 2016. “One Crop Breeding Cycle from Starvation? How Engineering Crop Photosynthesis for Rising CO 2 and Temperature Could Be One Important Route to Alleviation.” *Proceedings of the Royal Society B: Biological Sciences*.

Külheim, Carsten, Jon Ågren, and Stefan Jansson. 2002. “Rapid Regulation of Light Harvesting and Plant Fitness in the Field.” *Science*.

Long, S. P., S. Humphries, and P. G. Falkowski. 1994. “Photoinhibition of Photosynthesis in Nature.” *Annual Review of Plant Physiology and Plant Molecular Biology*.

Long, Stephen P., Xin Guang Zhu, Shawna L. Naidu, and Donald R. Ort. 2006. “Can Improvement in Photosynthesis Increase Crop Yields?” *Plant, Cell and Environment*.

Maxwell, Kate and Giles N. Johnson. 2000. “Chlorophyll Fluorescence - A Practical Guide.” *Journal of Experimental Botany*.

Meinke, David W., J. Michael Cherry, Caroline Dean, Steven D. Rounsley, and Maarten Koornneef. 1998. “Arabidopsis Thaliana: A Model Plant for Genome Analysis.” *Science*.

MONTEITH, J. 1977. “Climate and the Efficiency of Crop Production in Britain.” *Phil. Trans. R. Soc. Lond. B.*

Müller, P., X. P. Li, and K. K. Niyogi. 2001. “Non-Photochemical Quenching. A Response to Excess Light Energy.” *Plant Physiology*.

Murchie, Erik H. and Krishna K. Niyogi. 2011. “Manipulation of Photoprotection to Improve Plant Photosynthesis.” *Plant Physiology*.

Niyogi, Krishna K., Arthur R. Grossman, and Olle Björkman. 1998. “Arabidopsis Mutants Define a Central Role for the Xanthophyll Cycle in the Regulation of Photosynthetic

Energy Conversion.” *Plant Cell*.

Niyogi, Krishna K., Xiao Ping Li, Vanessa Rosenberg, and Hou Sung Jung. 2005. “Is PsbS the Site of Non-Photochemical Quenching in Photosynthesis?” in *Journal of Experimental Botany*.

Pérez-Bueno, Maria L., Matthew P. Johnson, Ahmad Zia, Alexander V. Ruban, and Peter Horton. 2008. “The Lhcb Protein and Xanthophyll Composition of the Light Harvesting Antenna Controls the ΔpH-Dependency of Non-Photochemical Quenching in Arabidopsis Thaliana.” *FEBS Letters* 582(10):1477–82.

Pessarakli, Mohammad. 2005. *Handbook of Photosynthesis*.

Ray, Deepak K., Nathaniel D. Mueller, Paul C. West, and Jonathan A. Foley. 2013. “Yield Trends Are Insufficient to Double Global Crop Production by 2050.” *PLoS ONE*.

Ruban, Alexander V. 2016. “Nonphotochemical Chlorophyll Fluorescence Quenching: Mechanism and Effectiveness in Protecting Plants from Photodamage.” *Plant Physiology*.

Schreiber, U., H. Hormann, C. Neubauer, and C. Klughammer. 1995. “Assessment of Photosystem II Photochemical Quantum Yield by Chlorophyll Fluorescence Quenching Analysis.” *Functional Plant Biology*.

Shikanai, Toshiharu, Yuri Munekage, Katsumi Shimizu, Tsuyoshi Endo, and Takashi Hashimoto. 1999. “Identification and Characterization of Arabidopsis Mutants with Reduced Quenching of Chlorophyll Fluorescence.” *Plant and Cell Physiology*.

Sinclair, Thomas R., Thomas W. Rufty, and Ramsey S. Lewis. 2019. “Increasing Photosynthesis: Unlikely Solution For World Food Problem.” *Trends in Plant Science* 24(11):1032–39.

Takahashi, Shunichi and Murray R. Badger. 2011. “Photoprotection in Plants: A New Light on Photosystem II Damage.” *Trends in Plant Science* 16(1):53–60.

Tietz, Stefanie, Christopher C. Hall, Jeffrey A. Cruz, and David M. Kramer. 2017. “NPQ(T): A Chlorophyll Fluorescence Parameter for Rapid Estimation and Imaging of Non-Photochemical Quenching of Excitons in Photosystem-II-Associated Antenna Complexes.” *Plant Cell and Environment* 40(8):1243–55.

Tilman, David, Christian Balzer, Jason Hill, and Belinda L. Befort. 2011. “Global Food Demand and the Sustainable Intensification of Agriculture.” *Proceedings of the National Academy of Sciences of the United States of America*.

Wang, Xiao Quan, David C. Tank, and Tao Sang. 2000. “Phylogeny and Divergence Times in Pinaceae: Evidence from Three Genomes.” *Molecular Biology and Evolution*.

Werner, Christiane, R. J. Ryel, O. Correia, and W. Beyschlag. 2001. “Effects of Photoinhibition on Whole-Plant Carbon Gain Assessed with a Photosynthesis Model.” *Plant, Cell and Environment*.

Zaks, Julia, Kapil Amarnath, David M. Kramer, Krishna K. Niyogi, and Graham R. Fleming. 2012. “A Kinetic Model of Rapidly Reversible Nonphotochemical Quenching.” *Proceedings of the National Academy of Sciences of the United States of America*.

Zhu, Xin-Guang, Stephen P. Long, and Donald R. Ort. 2010. “Improving Photosynthetic Efficiency for Greater Yield.” *Annual Review of Plant Biology*.

Zhu, Xin Guang, Donald R. Ort, John Whitmarsh, and Stephen P. Long. 2004. “The Slow Reversibility of Photosystem II Thermal Energy Dissipation on Transfer from High to

Low Light May Cause Large Losses in Carbon Gain by Crop Canopies: A Theoretical Analysis.” in *Journal of Experimental Botany*.

Appendix

Appendix 1: Photosynthetic parameters and their physiological meaning (Baker 2008)(Kramer et al. 2004)

Photosynthetic parameters	Formulas	Physiological meaning
Maximum quantum efficiency of PSII photochemistry	$(F_0-F_m)/F_m$	Maximum efficiency of the use of absorbed light by PSII in photochemistry
ϕPSII	$(F_p-F_{mp})/F_{mp}$	Estimation the efficiency of the photochemistry of PSII
NPQ	$(F_m/F_{mp})-1$	Estimation of the rate of light energy lost as heat by PSII
ϕNO	$1/(NPQ+1+qL*((F_m/F_0)-1))$ *$qL=((F_{mp}-F_p)/(F_m'-F_{0'}))*F_{0p}/F_p$	Reflects the non-light induced quenching process
qE	$(F_m/F_{mp})-(F_m/F_{mpp})$	Energy-dependent quenching, regulates the of excitation of PSII
qI	$(F_m-F_{mpp})/F_{mpp}$	Photo inhibitory quenching leads to photoinhibition in PSII
ϕNPQ	1-(ϕNO+ϕPSII)	The fraction of absorbed light dissipated by NPQ
NPQ(t)	$(4.88/((F'_m)/(F'_0)-1)))-1$	NPQ corrected for F_m
ϕNPQ(t)	1-(ϕNO(t)+ϕPSII)	ϕNPQ corrected for F_m
ϕNO(t)	1/(NPQ(t)+1+qL*4.88)	ϕNO corrected for F_m

Appendix 2: Light intensities time conversion table, for the fluctuating light response curve

For the fluctuating light response curve, the values of the photosynthetic parameters were not plotted against the light intensity but against the time. The corresponding time values are presented here. This correspondence is made in a way that the light intensity corresponds to the time of a protocol added to time of the previous protocol.

Light intensity (μmol m^{-2} s^{-1})	% use in the Robin program	Time correspondence (minutes)
65	12	15
131	16	30
129	15	45
259	24	60
191	19	75
383	32	90
250	23	105
500	39	120
304	27	135
605	46	150
354	30	165
707	52	180
397	33	195
793	58	210
433	35	225
866	62	240
462	37	255
924	66	270
483	38	285
966	68	300
496	39	315
991	70	330
500	40	345
1000	71	360

Appendix 3: The designs of the phenotyping experiments

The fluctuating light response curve

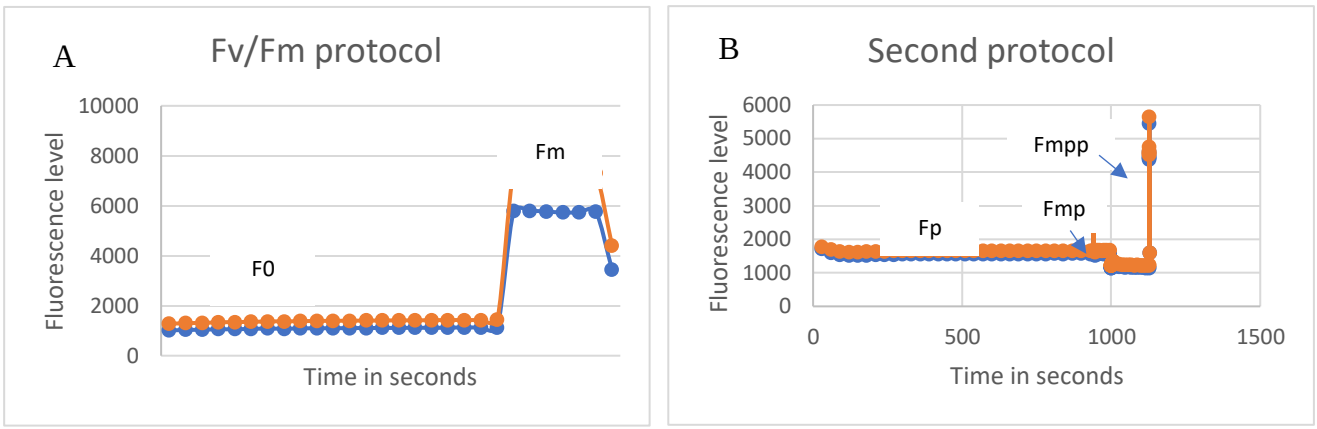

Figure 22: The level of chlorophyll fluorescence over the time. In the Fv/Fm protocol the level of fluorescence is minimal at the beginning and the maximal during the pulse. The second protocol consists in applying a certain intensity of actinic light at the beginning (from 65 to 1000 µmol m-2 s-1), according to this intensity the number of Q_A reduced or oxidized will not be the same, the level of the Fmp peak neither. After the Fmp peak, FAR red light is applied and second saturating pulse is applied(Fmpp). The second protocol is repeated for the 24 actinic light intensities described above.

The NPQ relaxation

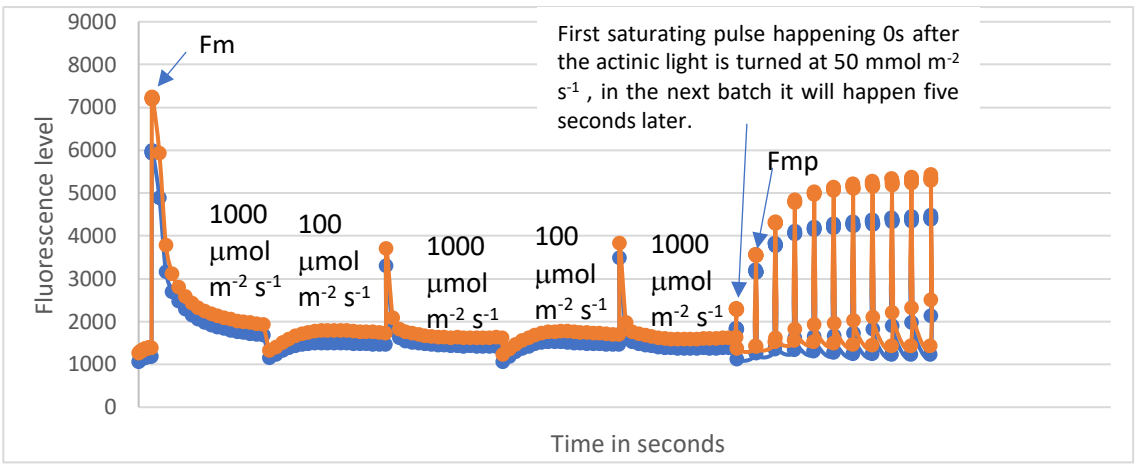

Figure 23: The NQP relaxation curve started with a Fv/Fm protocol to get the value of Fm essential to the calculation of NPQ. Then the intensity of the actinic light was fluctuated for fifteen minutes by alternating a period of three minutes of actinic light with an intensity of 1000 µmol m-2 s-1 with a period of 100 µmol m-2 s-1 for three minutes. In total three periods of three minutes at 1000 µmol m-2 s-1 and two periods of three minutes at 100 µmol m-2 s-1 were applied. Right after this period of fluctuating light, actinic light was turned on at 50 µmol m-2 s-1 and saturating pulses were applied every thirty seconds for five minutes. In this figure the first saturating pulse of the period of relaxation happens simultaneously as the actinic light of 50 µmol m-2 s-1 is turned on. On the figure representing the NPQ relaxation of the other batches, the first pulse would have been shifted respectively of five, ten, fifteen, twenty, twenty-five seconds compared to the first pulse of this batch.

Appendix 4: The cytoplasmic swap panel

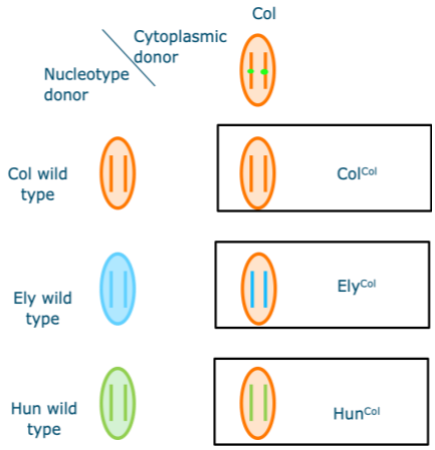

Figure 24: Reciprocal crosses between Ely, Col, and Hun. Col CENH3-1 *mutant is used a cytoplasmic donor, while Ely, Hun and Col WT are used as nucleotype donor. The nucleotype donor is the male while the plasmotype donor is the male. The genome of Ely is represented in blue, the genome of Col is represented in orange and the genome of hu is represented in green.*

Appendix 5: additional figures

- ϕPSII through all light intensities (fluctuating light response curve data)

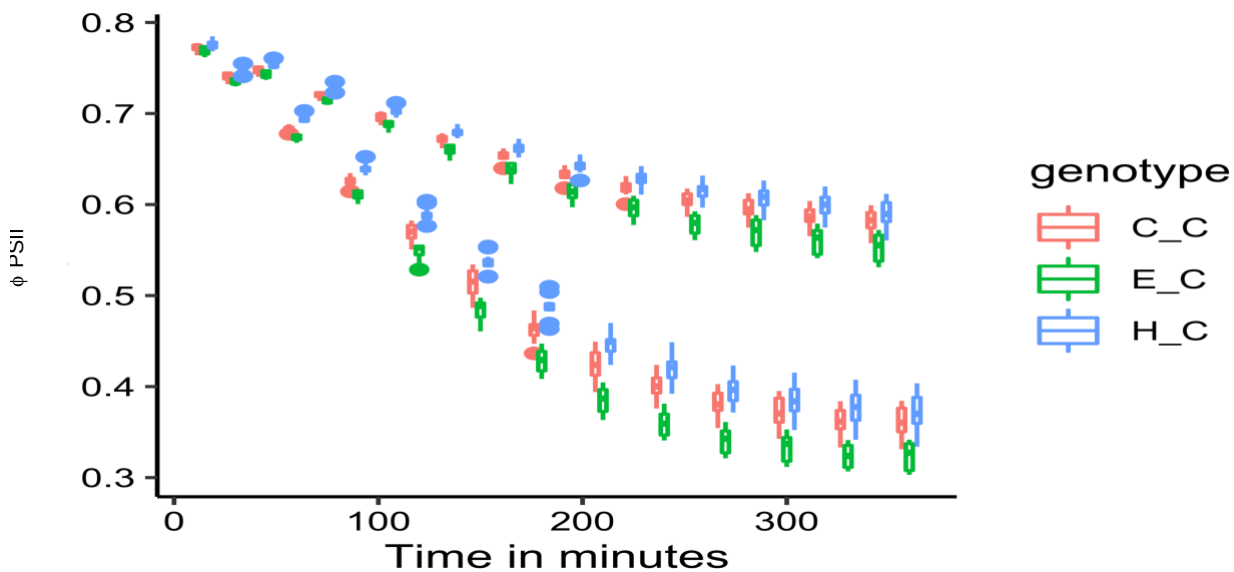

Figure 25: The rate of ϕPSII decreases with the actinic light intensity increase. The boxes of this figure can be read as the boxes of the figures 7. In this figure the blue boxes represent the

value of ϕPSII for the cybrid Hun_{Col} , the red boxes the value of ϕPSII for the cybrid Col_{Col}, and green boxes the value of ϕPSII for the cybrid Ely_{Col} . Each group of blue, red and green boxes represent the values of qI of the three cybrids for a certain light intensity. The first group of boxes on the left represent the values of ϕPSII when the actinic light intensity was 65 µmol. m^{-2}. s^{-1}, and this until 1000 µmol. m^{-2}. s^{-1}.

- ϕPSII p-value for all light intensities (fluctuating light response curve data)

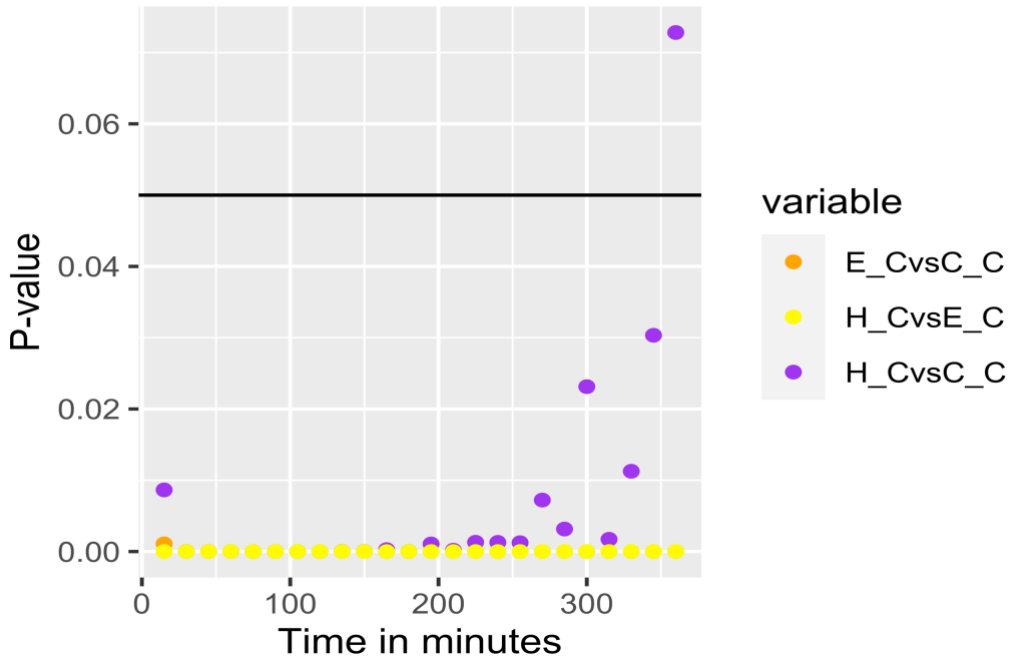

Figure 26: This figure represents the result of the posthoc test for the variations of ϕPSII between the cybrids . The black line represents the risk α fixed here at 0.05. The dots represent the adjusted Tukey p-value obtained from the posthoc test. Each column of dots represents one posthoc test for the three cybrids , per time point so per light intensity. The first column on the left corresponds to the adjusted Tukey p-value of the posthoc test when the light intensity is 65µmol. m^{-2}. s^{-1}, and then this pattern continues until 1000 µmol. m^{-2}. s^{-1}. The yellow dots are for the comparison Hun_{Col} VS Ely_{Col}, the orange for Ely_{Col} VS Col_{Col}, and the purple one for Hun_{Col} VS Col_{Col}.

- ϕNO through all light intensities (fluctuating light response curve data)

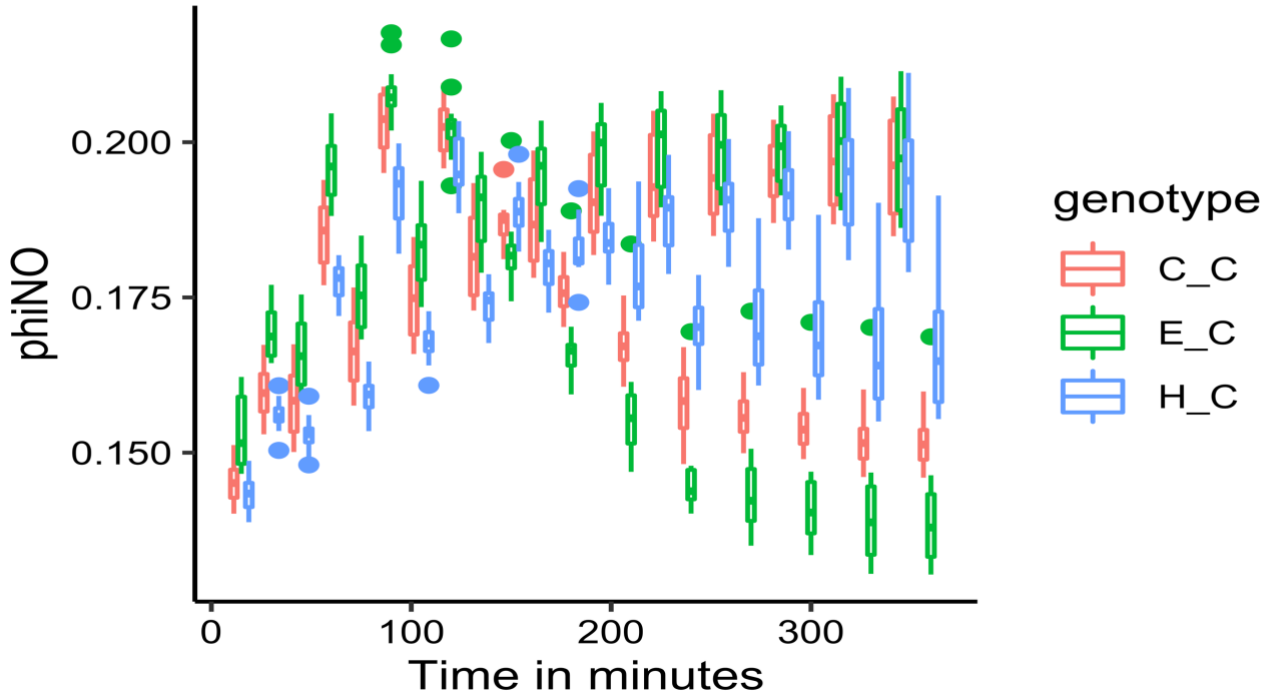

Figure 27: The rate of ϕNO(phiNO) decreases at high light intensities (after 793 µmol. m-2. s-1). The difference of ϕNO between the cybrids also increase when the light intensity increases. The boxes of this figure can be read as the boxes of the figure 7. In this figure the blue boxes represent the value of ϕNO for the cybrid Hun$_{Col}$, the red boxes the value of ϕNO for the cybrid Col$_{Col}$, and green boxes the value of ϕNO for the cybrid Ely$_{Col}$. Each group of blue, red and green boxes represent the values of ϕNO of the three cybrids for a certain light intensity. The first group on the left represent the values of ϕNO when the actinic light intensity was 65 µmol. m-2. s-1, and this until 1000 µmol. m-2. s-1.

- ϕNO p-value for all light intensities (fluctuating light response curve data)

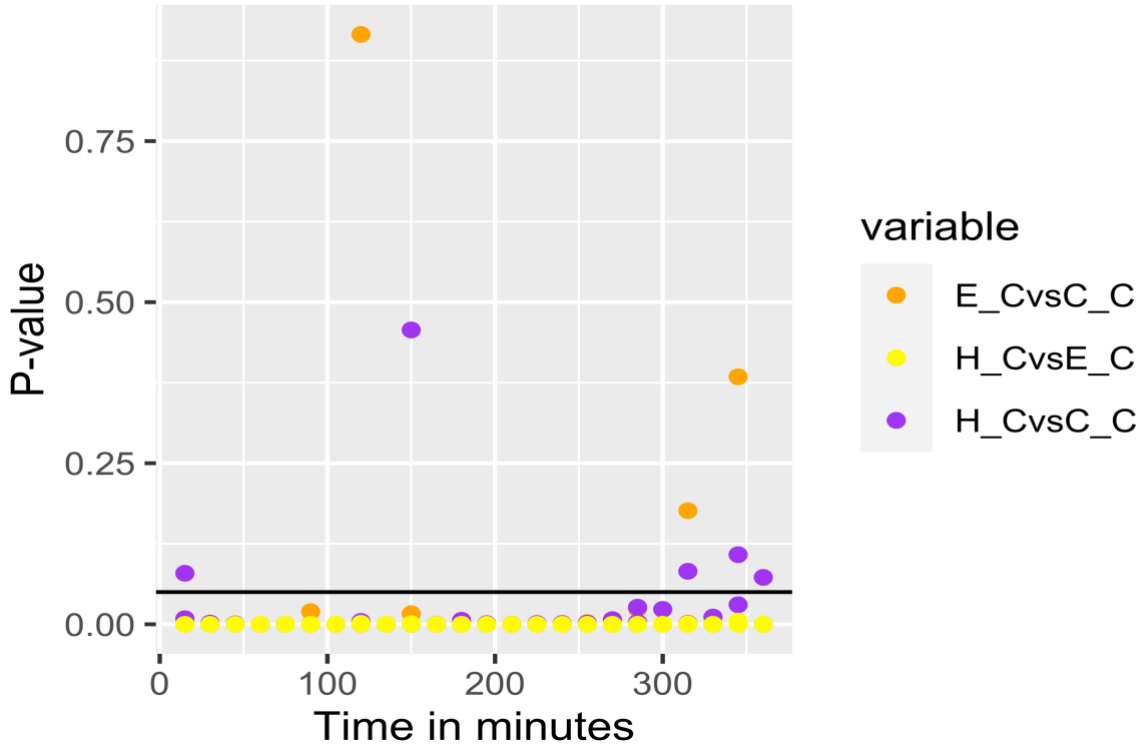

Figure 28: This figure represents the results posthoc test with the adjusted Tukey p-value for the variations of ϕNO for the subset of high light intensities and between the cybrids . The black line represents the risk α fixed here at 0.05. The dots represent the adjusted Tukey p-value obtained from the posthoc test. Each column of dots represents one posthoc test for the three cybrids , per time point so per light intensity. The first column on the left corresponds to the adjusted Tukey p-value of the posthoc test when the light intensity is 605 µmol. m^{-2}. s^{-1}, and then this pattern continues until 1000 µmol. m^{-2}. s^{-1}. The yellow dots are for the comparison Hun_{Col} VS Ely_{Col}, the orange for Ely_{Col} VS Col_{Col}, and the purple one for Hun_{Col} VS Col_{Col}.

- ϕNPQ through all light intensities (fluctuating light response curve data)

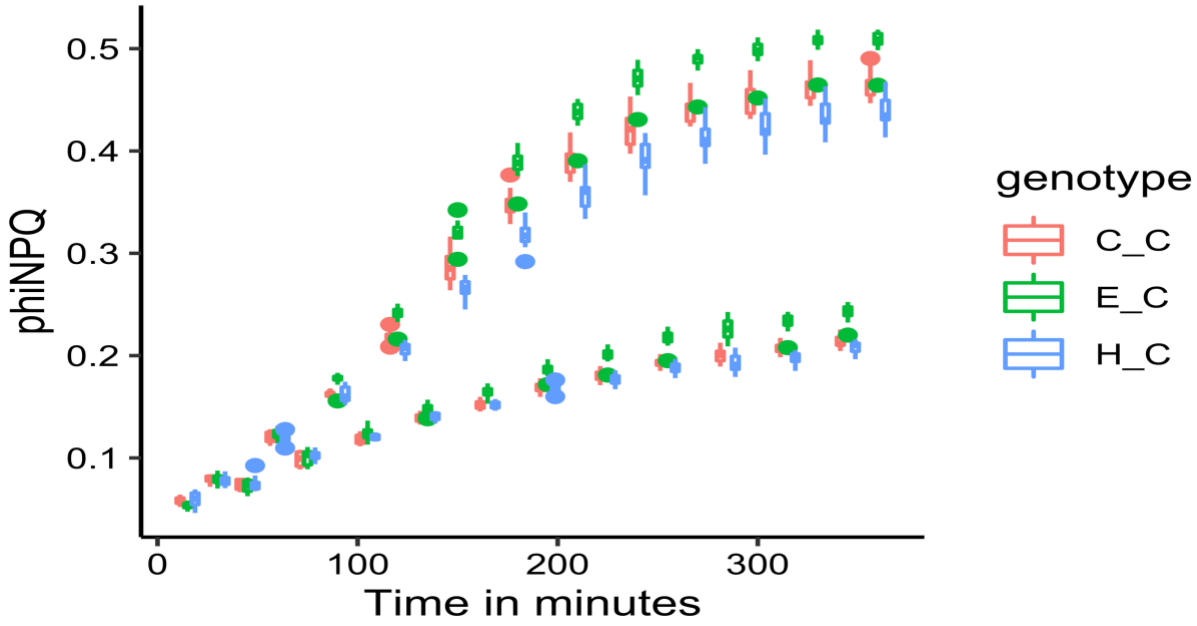

Figure 29: The rate of ϕNPQ(phiNPQ) increases when light intensity increases. The difference of ϕNPQ between the cybrids also increase when the light intensity increases. The boxes of this figure can be read as the boxes of the figure 7. In this figure the blue boxes represent the value of ϕNPQ for the cybrid Hun$_{Col}$, the red boxes the value of ϕNPQ for the cybrid Col$_{Col}$, and green boxes the value of ϕNPQ for the cybrid Ely$_{Col}$. Each group of blue, red and green boxes represent the values of qI of the three cybrids for a certain light intensity. The first group on the left represent the values of ϕNPQ when the actinic light intensity was 65 µmol. m^{-2}. s^{-1}, and this until 1000 µmol. m^{-2}. s^{-1}.

- ϕNPQ p-value for all light intensities (fluctuating light response curve data)

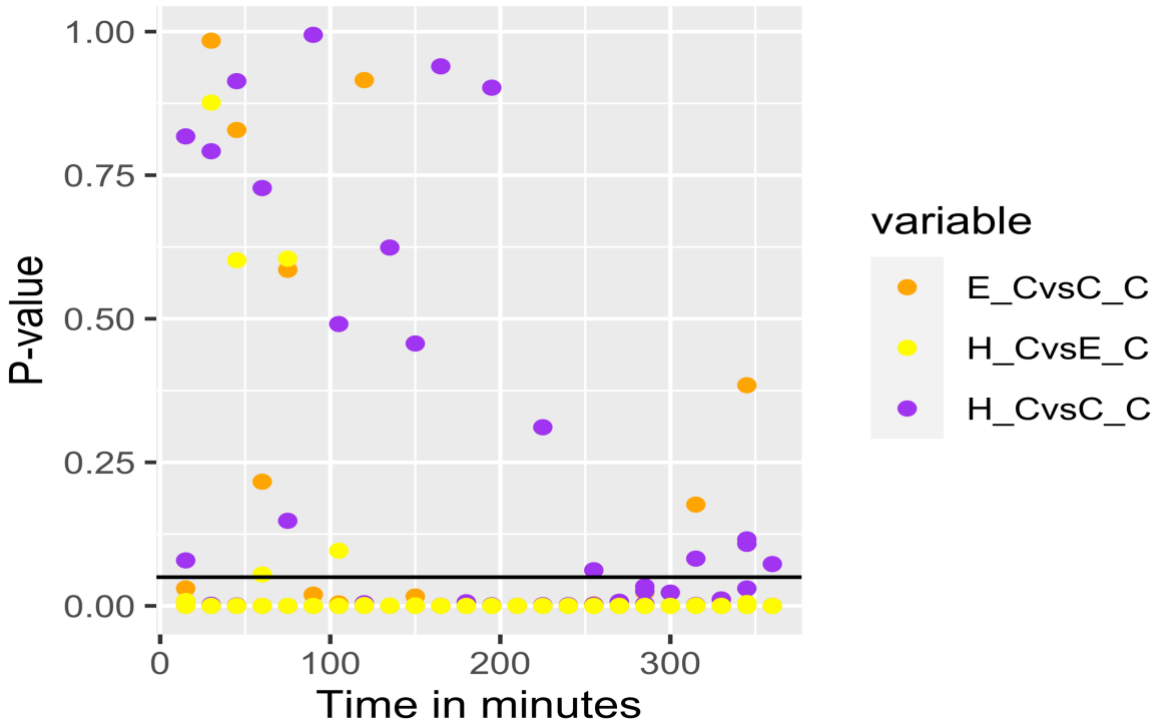

Figure 30: This figure represents the results posthoc test with the adjusted Tukey p-value for the variations of ϕNPQ for the subset of high light intensities and between the cybrids. The black line represents the risk α fixed here at 0.05. The dots represent the adjusted Tukey p-value obtained from the posthoc test. Each column of dots represents one posthoc test for the three cybrids , per time point so per light intensity. The first column on the left corresponds to the adjusted Tukey p-value of the posthoc test when the light intensity is 605 µmol. m^{-2}. s^{-1}, and then this pattern continues until 1000 µmol. m^{-2}. s^{-1}. The yellow dots are for the comparison Hun_{Col} VS Ely_{Col}, the orange for Ely_{Col} VS Col_{Col}, and the purple one for Hun_{Col} VS Col_{Col}.

- NPQ normalized (NPQ relaxation data)

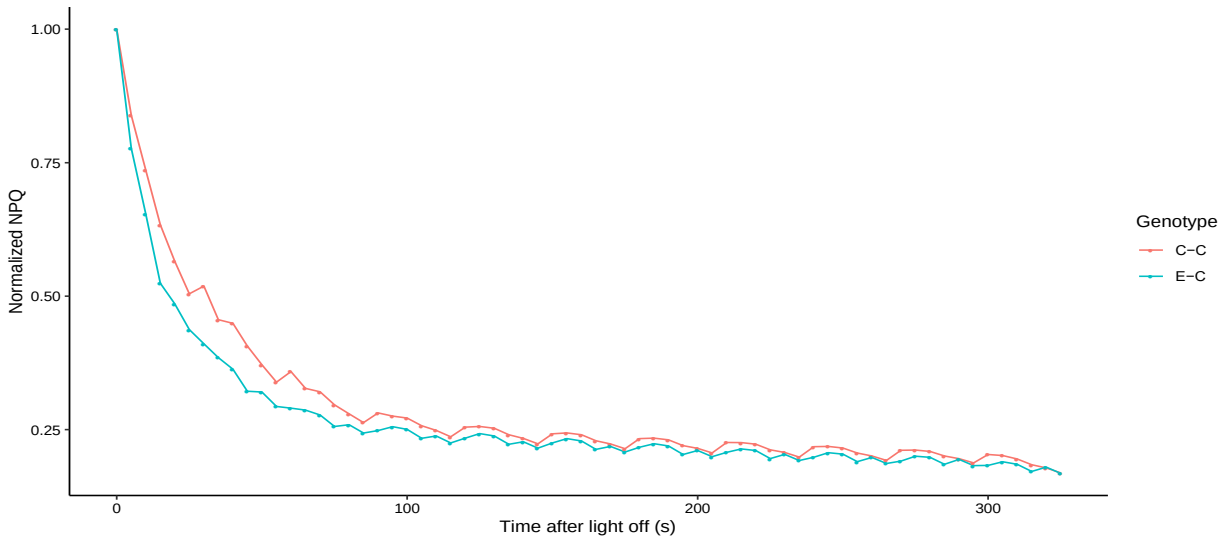

Figure 31: The normalized relaxation NPQ at low light intensity of through the time (after fifteen minutes of fluctuation of 1000 and 100 µmol. m-2. s- (cf. Appendix 3, figure 21)) is represented here, the results of all the batches are combined. To normalize the value of NPQ, we have done the ratio the value of NPQ from 1 to n above the first value of NPQ. Each dot is then normalized the value of NPQ averaged over of the individual value NPQ of the ten plants of each cybrids. The red line is for Col$_{Col}$, the blue line is for Ely$_{Col}$.

- ϕPSII normalized (NPQ relaxation data)

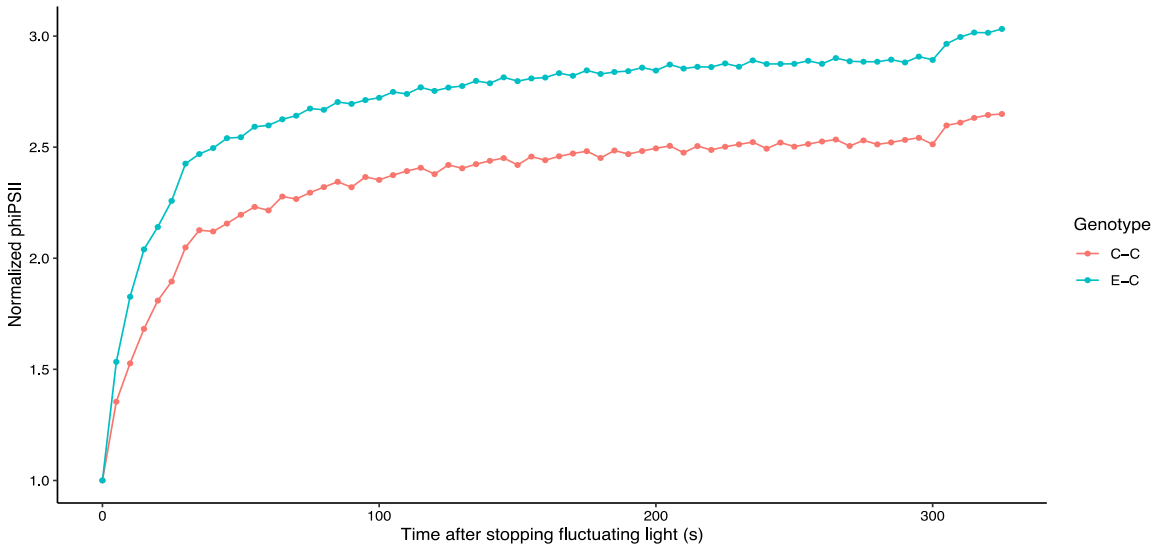

Figure 32: The normalized increase of ϕPSII through the time (after fifteen minutes of fluctuation of 1000 and 100 µmol. m-2. s- (cf. Appendix 3, figure 21)) is represented here, the results of all the batches are combined. To normalize the value of ϕPSII, we have done the ratio the value of ϕPSII from 1 to n above the first value of ϕPSII. Each dot is then normalized

the value of ϕPSII averaged over of the individual value ϕPSII of the ten plants of each cybrids. The red line is for Col$_{Col}$, the blue line is for Ely$_{Col}$.

- NPQ relaxation in the dark after a period of fifteen minutes of light fluctuation (NPQ dark relaxation data)

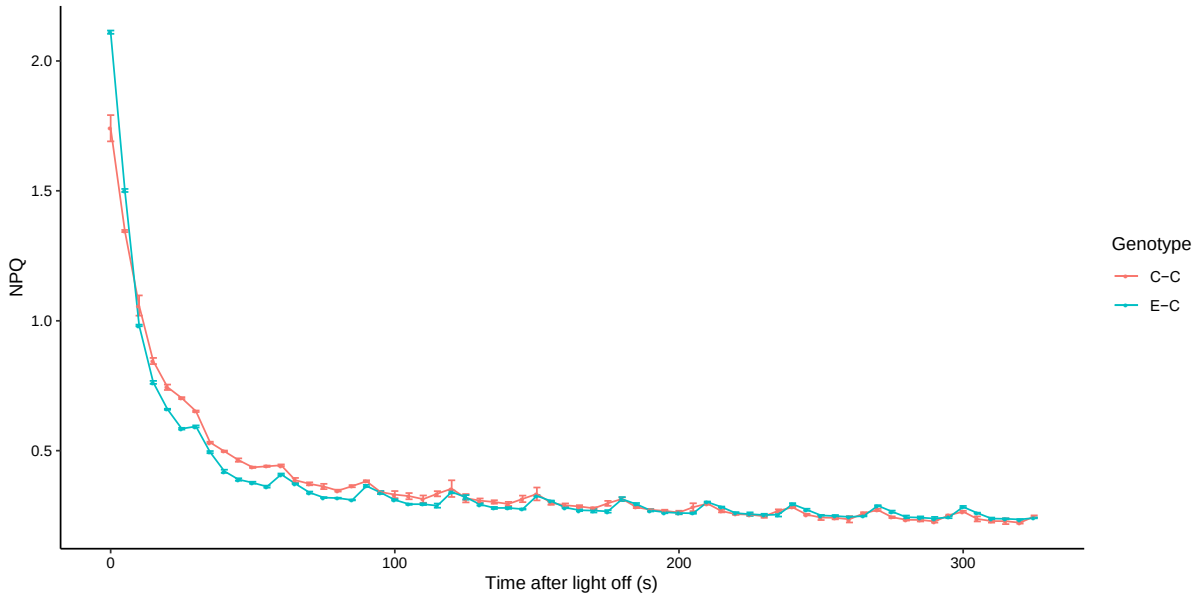

Figure 33: The relaxation NPQ in the dark of through the time (after fifteen minutes of fluctuation of 1000 and 100 µmol. m^{-2}. s^{-} (cf. Appendix 3, figure 21)) is represented here. The results of all the batches are combined. The red line is for Col$_{Col}$, the blue line is for Ely$_{Col}$.

- Normalized NPQ relaxation in the dark after a period of fifteen minutes of light fluctuation (NPQ dark relaxation data)

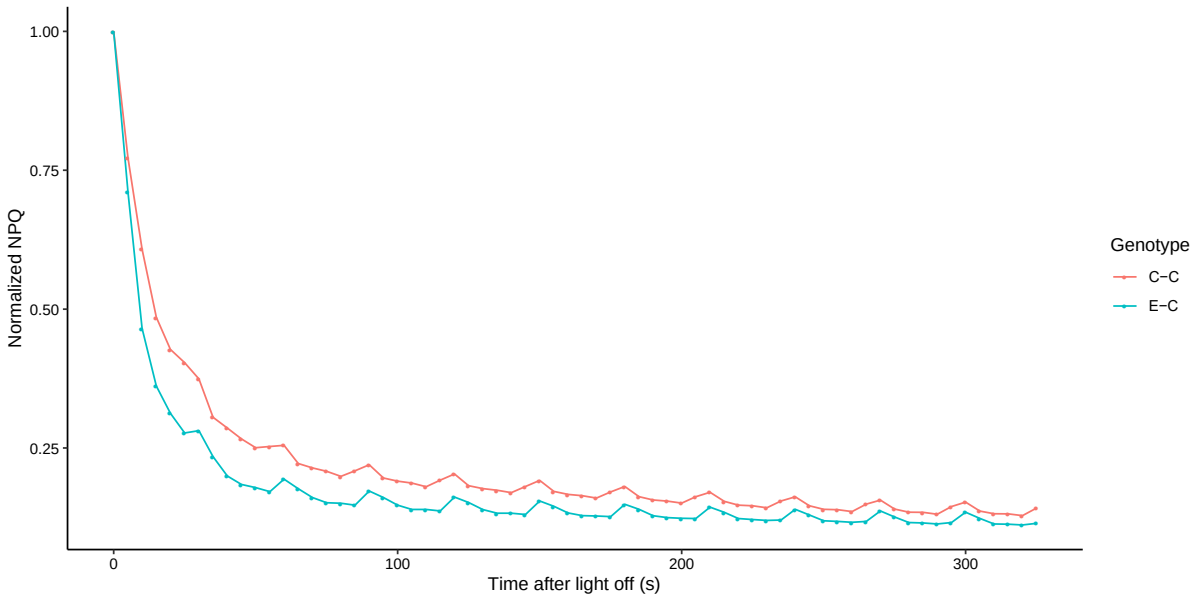

Figure 34: The normalized relaxation NPQ in the dark of through the time (after fifteen minutes of fluctuation of 1000 and 100 µmol. m-2. s- (cf. Appendix 3, figure 21)) is represented here, the results of all the batches are combined. To normalize the value of NPQ, we have done the ratio the value of NPQ from 1 to n above the first value of NPQ. Each dot is then normalized the value of NPQ averaged over of the individual value NPQ of the ten plants of each cybrids. The red line is for Col$_{Col}$, the blue line is for Ely$_{Col}$.

- ANOVA per time point for the NPQ relaxation in the dark (NPQ dark relaxation data)

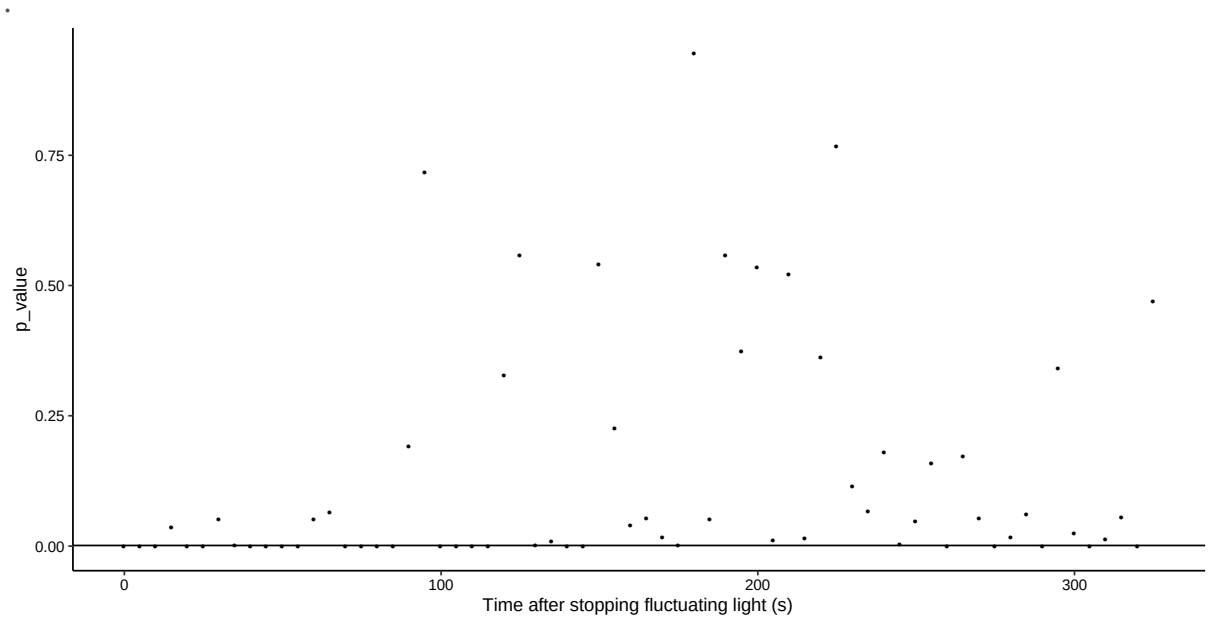

Figure 35:The results of the one-way ANOVA conducted per time point for the difference of NPQ between Col_{Col} and Ely_{Col} are represented here. The black line represents the risk α fixed here at 0.05. The difference of NPQ between the two cybrids is almost always significantly different for the first hundred-fifty seconds.

- NPQ variations (fluctuating light response curve)

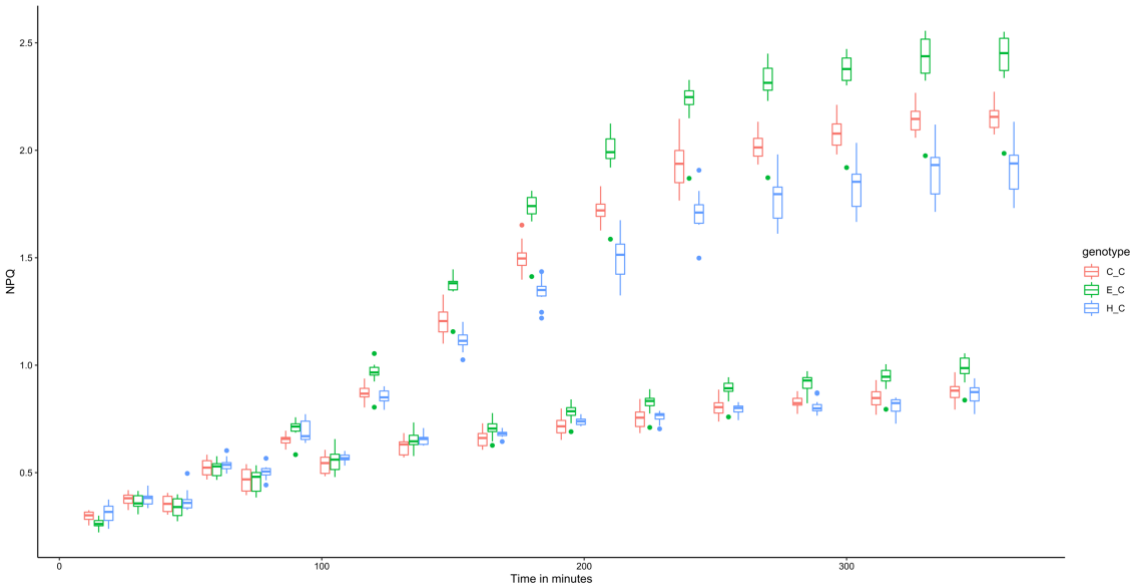

Figure 36: NPQ increases with the actinic light intensity increase. Each group of blue, red and green boxes represent the values of NPQ of the three cybrids for a certain light intensity. The orange boxes are for Col$_{Col}$, the green boxes for Ely$_{Col}$, the blue boxes for Hun$_{Col}$. The first group on the left represent the values of NPQ when the actinic light intensity was 65 µmol. m^{-2}. s^{-1}, and this until 1000 µmol. m^{-2}. s^{-1}.

- Posthoc test on NPQ variations (fluctuating light response curve)

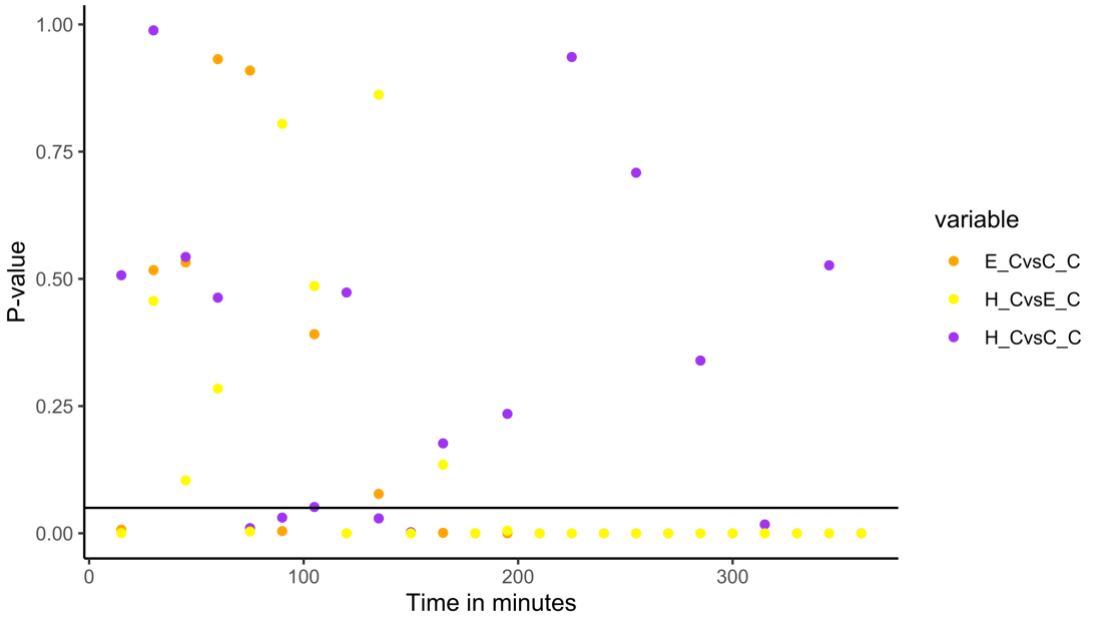

Figure 37: This figure represents the result of the posthoc test, with Tukey p-value adjustment, for the variations of NPQ between the cybrids . The black line represents α threshold of 0.05. The dots represent the adjusted Tukey p-value obtained from the posthoc test. Each column of dots represents the results of one posthoc test for the three cybrids, per time point so per light intensity. The first column on the left corresponds to the results of the posthoc test when the light intensity is 65 µmol. m^{-2}. s^{-1}, and then this pattern continues until 1000 µmol. m^{-2}. s^{-1}. The yellow dots are for the comparison Hun_{Col} VS Ely_{Col}, the orange for Ely_{Col} VS Col_{Col}, and the purple one for Hun_{Col} VS Col_{Col}.

Appendix 6: Statistics

- The linear correlation between NPQ and NPQt (summary of the linear model)

all:
lm(formula = NPQt ~ NPQ, data = NPQvsNPQt_final)

Residuals:
    Min   1Q Median   3Q   Max
-2.2954 -0.7218 -0.2114 0.5527 7.4472

Coefficients:
             Estimate Std. Error t value Pr(>|t|)
(Intercept) -1.47568   0.07405 -19.93   <2e-16 ***
NPQ   5.14982   0.05989   85.98   <2e-16 ***

Signif. codes: 0 ‘***’ 0.001 ‘**’ 0.01 ‘*’ 0.05 ‘.’ 0.1 ‘ ’ 1

Residual standard error: 1.182 on 958 degrees of freedom
Multiple R-squared: 0.8853, Adjusted R-squared: 0.8852

F-statistic: 7393 on 1 and 958 DF, p-value: < 2.2e-16

- The linear correlation between qE and NPQ(t) (summary of the linear model)

```
Call:
lm(formula = qE ~ value, data = qE_subset)

Residuals:
    Min      1Q  Median      3Q     Max
-0.39270 -0.04954 -0.01276  0.03561  0.28340

Coefficients:
             Estimate Std. Error t value Pr(>|t|)
(Intercept) -0.050024   0.008208  -6.094 3.03e-09 ***
value        0.389099   0.003675 105.866  < 2e-16 ***
---
Signif. codes:  0 ‘***’ 0.001 ‘**’ 0.01 ‘*’ 0.05 ‘.’ 0.1 ‘ ’ 1

Residual standard error: 0.104 on 334 degrees of freedom
Multiple R-squared:  0.9711, Adjusted R-squared:  0.971
F-statistic: 1.121e+04 on 1 and 334 DF,  p-value: < 2.2e-16
```

- The non-linear correlation between qI and NPQ(t) (summary of the linear model)

```
Call:
lm(formula = qI ~ value, data = NPQt_qI)

Residuals:
    Min      1Q  Median      3Q     Max
-0.29996 -0.06165  0.01545  0.08152  0.28618

Coefficients:
             Estimate Std. Error t value Pr(>|t|)
(Intercept)  3.479e-01  5.009e-03   69.45   <2e-16 ***
value       -2.079e-04  1.242e-05  -16.74   <2e-16 ***
---
Signif. codes:  0 ‘***’ 0.001 ‘**’ 0.01 ‘*’ 0.05 ‘.’ 0.1 ‘ ’ 1

Residual standard error: 0.1209 on 958 degrees of freedom
Multiple R-squared:  0.2263, Adjusted R-squared:  0.2255
F-statistic: 280.3 on 1 and 958 DF,  p-value: < 2.2e-16
```

- The results of the ANOVA and Tukey analysis for NPQt
    - One-way ANOVA

Type III Analysis of Variance Table with Satterthwaite's method

```
        Sum Sq Mean Sq NumDF DenDF F value    Pr(>F)
cybrid 16.634  8.3171     2    36  83.012 3.282e-14 ***
---
Signif. codes:  0 ‘***’ 0.001 ‘**’ 0.01 ‘*’ 0.05 ‘.’ 0.1 ‘ ’ 1
```

- Tukey test

```
$`emmeans of cybrid`
 cybrid emmean    SE   df lower.CL upper.CL
 C_C       3.46 0.244 1.18   -2.041     8.97
 E_C       4.65 0.244 1.18   -0.853    10.16
 H_C       3.16 0.246 1.22   -1.824     8.15

Degrees-of-freedom method: kenward-roger
Confidence level used: 0.95
Conf-level adjustment: sidak method for 3 estimates

$`pairwise differences of cybrid`
 contrast  estimate    SE df t.ratio p.value
 C_C - E_C   -1.188 0.120 36 -9.932  <.0001
 C_C - H_C    0.302 0.125 36  2.427  0.0519
 E_C - H_C    1.491 0.125 36 11.970  <.0001

Degrees-of-freedom method: kenward-roger
P value adjustment: tukey method for comparing a family of 3 estimates
```

- The results of the Tukey analysis for the slopes and intercepts between NPQt and FqFm

  - Slopes

```
$`emmeans of Cybrid`
 Cybrid emmean    SE   df lower.CL upper.CL
 C_C      -6.73 0.219 1.20    -11.5    -2.00
 E_C      -7.60 0.219 1.20    -12.3    -2.86
 H_C      -6.12 0.221 1.25    -10.4    -1.86

Degrees-of-freedom method: kenward-roger
Confidence level used: 0.95
Conf-level adjustment: sidak method for 3 estimates

$`pairwise differences of Cybrid`
 contrast  estimate    SE df t.ratio p.value
 C_C - E_C    0.862 0.112 36   7.689 <.0001
 C_C - H_C   -0.612 0.117 36  -5.248 <.0001
 E_C - H_C   -1.474 0.117 36 -12.635 <.0001

Degrees-of-freedom method: kenward-roger
```

P value adjustment: tukey method for comparing a family of 3 estimates

- Intercepts

`emmeans of Cybrid`
 Cybrid emmean SE df lower.CL upper.CL
 C_C 4.49 0.0918 1.27 2.79 6.18
 E_C 4.84 0.0918 1.27 3.14 6.54
 H_C 4.22 0.0931 1.34 2.73 5.72

Degrees-of-freedom method: kenward-roger
Confidence level used: 0.95
Conf-level adjustment: sidak method for 3 estimates

$`pairwise differences of Cybrid`
 contrast estimate SE df t.ratio p.value
 C_C - E_C -0.351 0.0539 36 -6.516 <.0001
 C_C - H_C 0.262 0.0561 36 4.678 0.0001
 E_C - H_C 0.613 0.0561 36 10.938 <.0001

Degrees-of-freedom method: kenward-roger
P value adjustment: tukey method for comparing a family of 3 estimates

- The results of the ANOVA and Tukey analysis for qE

- One-way ANOVA

Type III Analysis of Variance Table with Satterthwaite's method
 Sum Sq Mean Sq NumDF DenDF F value Pr(>F)
cybrid 1.3094 0.65469 2 36.996 66.981 5.055e-13 ***

Signif. codes: 0 ‘***’ 0.001 ‘**’ 0.01 ‘*’ 0.05 ‘.’ 0.1 ‘ ’ 1

- Tukey test

$`emmeans of cybrid`
 cybrid emmean SE df lower.CL upper.CL
 C_C 1.41 0.0264 7.45 1.33 1.49
 E_C 1.66 0.0264 7.45 1.58 1.74
 H_C 1.21 0.0285 9.65 1.13 1.29

Degrees-of-freedom method: kenward-roger
Confidence level used: 0.95
Conf-level adjustment: sidak method for 3 estimates

$`pairwise differences of cybrid`
 contrast estimate SE df t.ratio p.value
 C_C - E_C -0.246 0.0374 36 -6.581 <.0001

C_C - H_C 0.202 0.0389 36 5.189 <.0001
E_C - H_C 0.448 0.0389 36 11.512 <.0001

Degrees-of-freedom method: kenward-roger
P value adjustment: tukey method for comparing a family of 3 estimates

- The results of the ANOVA and Tukey analysis for qI

  - One-way ANOVA

Type III Analysis of Variance Table with Satterthwaite's method
Sum Sq Mean Sq NumDF DenDF F value Pr(>F)
cybrid 0.023644 0.011822 2 36 20.52 1.128e-06 ***

Signif. codes: 0 '***' 0.001 '**' 0.01 '*' 0.05 '.' 0.1 ' ' 1

  - Tukey test

$`emmeans of cybrid`
cybrid emmean SE df lower.CL upper.CL
C_C 0.557 0.0272 1.08 -0.245 1.36
E_C 0.576 0.0272 1.08 -0.225 1.38
H_C 0.517 0.0273 1.10 -0.244 1.28

Degrees-of-freedom method: kenward-roger
Confidence level used: 0.95
Conf-level adjustment: sidak method for 3 estimates

$`pairwise differences of cybrid`
contrast estimate SE df t.ratio p.value
C_C - E_C -0.0195 0.00907 36 -2.153 0.0934
C_C - H_C 0.0402 0.00944 36 4.258 0.0004
E_C - H_C 0.0597 0.00944 36 6.326 <.0001

Degrees-of-freedom method: kenward-roger
P value adjustment: Tukey method for comparing a family of 3 estimates

Appendix 7: Batches design

- Fluctuating light response curve

Hun_{Col}	Ely_{Col}	Hun_{Col}	Ely_{Col}	Hun_{Col}	D
Ely_{Col}	Col_{Col}	Ely_{Col}	Col_{Col}	Ely_{Col}	C
Hun_{Col}	Ely_{Col}	Col_{Col}	Col_{Col}	Col_{Col}	B
Hun_{Col}	Ely_{Col}	Col_{Col}	Col_{Col}	Hun_{Col}	A
5	4	3	2	1	

- NPQ relaxation

Col_{Col}	Ely_{Col}	Col_{Col}	Ely_{Col}	Col_{Col}	D
Ely_{Col}	Col_{Col}	Ely_{Col}	Col_{Col}	Ely_{Col}	C
Col_{Col}	Ely_{Col}	Col_{Col}	Ely_{Col}	Col_{Col}	B
Ely_{Col}	Col_{Col}	Ely_{Col}	Col_{Col}	Ely_{Col}	A
5	4	3	2	1	

Appendix 7: NPQ relaxation script for the PSI PlantScreen Module

S=50ms
;protocol body - new protocol
;version PK May 1, 2007
include default.inc ;Includes standard options, do not remove it !
include light.inc ;Includes standard options, do not remove it !

;NPQ relaxation protocol

__LightA=0

__LightB=0

__Lightintensity =<17,75>

Shutter=3

Sensitivity=1

Super=100

FAR=20

;*** F0 Measurement ***

F0Duration=20s;

F0measurement =1s

a1=0s

a2=a1+F0Duration

<a1,a1+F0measurement..a2>=>mfmsub

<a1>=>checkPoint,"startFo"

<a1+F0Duration>=>checkPoint,"endFo"

;*** Saturating Pulse & Fm Measurement ******************************

PulseDuration=800ms; ##

a2=a1+F0Duration

a3=a2+400ms

;

<a2>=>SatPulse(PulseDuration)

<a2>=>mpulse2

<a2>=>checkPoint,"startFm_Lss"

<a2 + PulseDuration >=>checkPoint,"endFm_Lss"

<a3>=>checkPoint,"timeVisual"

;

;*** Light fluctuation 2000/200 uE**

Highlightperiod1=182s

Highlightperiod=180s

Hightlightmeasurement=10s

lowlightperiod=180s

lowlightmeasurement=10s

relaxactlight=300s

a4=a2+PulseDuration+1200ms

a5=a4+Highlightperiod

a6=a5+lowlightperiod

a7=a6+Highlightperiod

a8=a7+lowlightperiod

a9=a8+Highlightperiod

a10=a8+Highlightperiod +25s

<a2-TS>=>SI_Act2(75)

<a2>=>act2(Highlightperiod1)

<a4,a4+Hightlightmeasurement..a4+Highlightperiod>=>mfmsub

<a5-TS>=>SI_Act2(17)

<a5>=>act2(lowlightperiod)

<a5 +TS,a5+lowlightmeasurement..a5+lowlightperiod>=>mfmsub

<a6-TS>=>SI_Act2(75)

<a6>=>act2(Highlightperiod)

<a6 +TS,a6+Hightlightmeasurement..a6+Highlightperiod>=>mfmsub

<a7-TS>=>SI_Act2(17)

<a7>=>act2(lowlightperiod)

<a7+TS,a7+lowlightmeasurement..a7+lowlightperiod>=>mfmsub

<a8-TS>=>SI_Act2(75)

<a8>=>act2(Highlightperiod)

<a8 +TS,a8+Hightlightmeasurement..a8+Highlightperiod>=>mfmsub

;********** relaxation's monitoring**********

<a9>=>SI_Act2(10)

<a9>=>act2(relaxactlight)

<a10>=>SatPulse(PulseDuration)

<a10>=>mpulse2

<a10>=>checkPoint,"startFm_Lss"

<a10 + PulseDuration >=>checkPoint,"endFm_Lss"

<a10>=>checkPoint,"timeVisual"

a11=a10+30s

<a11>=>SatPulse(PulseDuration)

<a11>=>mpulse2

<a11>=>checkPoint,"startFm_Lss"

<a11 + PulseDuration >=>checkPoint,"endFm_Lss"

<a11>=>checkPoint,"timeVisual"

a12=a11+30s

<a12>=>SatPulse(PulseDuration)

<a12>=>mpulse2

<a12>=>checkPoint,"startFm_Lss"

<a12 + PulseDuration >=>checkPoint,"endFm_Lss"

<a12>=>checkPoint,"timeVisual"

a13=a12+30s

<a13>=>SatPulse(PulseDuration)

<a13>=>mpulse2

<a13>=>checkPoint,"startFm_Lss"

<a13 + PulseDuration >=>checkPoint,"endFm_Lss"

<a13>=>checkPoint,"timeVisual"

a14=a13+30s

<a14>=>SatPulse(PulseDuration)

<a14>=>mpulse2

<a14>=>checkPoint,"startFm_Lss"

<a14 + PulseDuration >=>checkPoint,"endFm_Lss"

<a14>=>checkPoint,"timeVisual"

a15=a14+30s

<a15>=>SatPulse(PulseDuration)

<a15>=>mpulse2

<a15>=>checkPoint,"startFm_Lss"

<a15 + PulseDuration >=>checkPoint,"endFm_Lss"

<a15>=>checkPoint,"timeVisual"

a16=a15+30s

<a16>=>SatPulse(PulseDuration)

<a16>=>mpulse2

<a16>=>checkPoint,"startFm_Lss"

<a16 + PulseDuration >=>checkPoint,"endFm_Lss"

<a16>=>checkPoint,"timeVisual"

a17=a16+30s

<a17>=>SatPulse(PulseDuration)

<a17>=>mpulse2

<a17>=>checkPoint,"startFm_Lss"

<a17 + PulseDuration >=>checkPoint,"endFm_Lss"

<a17>=>checkPoint,"timeVisual"

a18=a17+30s

<a18>=>SatPulse(PulseDuration)

<a18>=>mpulse2

<a18>=>checkPoint,"startFm_Lss"

<a18 + PulseDuration >=>checkPoint,"endFm_Lss"

<a18>=>checkPoint,"timeVisual"

a19=a18+30s

<a19>=>SatPulse(PulseDuration)

<a19>=>mpulse2

<a19>=>checkPoint,"startFm_Lss"

<a19 + PulseDuration >=>checkPoint,"endFm_Lss"

<a19>=>checkPoint,"timeVisual"

a20=a19+30s

<a20>=>SatPulse(PulseDuration)

<a20>=>mpulse2

<a20>=>checkPoint,"startFm_Lss"

<a20 + PulseDuration >=>checkPoint,"endFm_Lss"

<a20>=>checkPoint,"timeVisual"